

# Network Induced Large Correlation Matrix Estimation

Shuo Chen<sup>1\*</sup>, Jian Kang<sup>2</sup>, Yishi Xing<sup>1</sup>, Yunpeng Zhao<sup>3</sup>, and Donald Milton<sup>4</sup>

<sup>1</sup> Department of Epidemiology and Biostatistics, University of Maryland, College Park, MD 20742, USA

<sup>2</sup> Department of Biostatistics, University of Michigan, Ann Arbor, MI 48109, USA

<sup>3</sup> Department. of Statistics, George Mason University, Fairfax, VA 22030, USA

<sup>4</sup> Maryland Institute for Applied Environmental Health, University of Maryland, College Park, MD 20742, USA

## Abstract

We consider to estimate community network induced large correlation matrices. The correlation matrix of massive biomedical data (e.g. gene expression or neuroimaging) often exhibits a complex and organized, yet latent graph topological structure. Although current regularization methods using thresholding or shrinkage strategies may provide satisfactory estimation of the large covariance/correlation and precision matrices, they do not allow automatically detecting the latent graph topological structures nor integrating the topological information into correlation matrix estimation. In this paper, we show that uncovering the latent topological structure of the correlation matrix provides informative prior knowledge for the regularization step and allows edges to borrow strength from each other properly. Therefore, we propose a two step procedure that seamlessly detects the latent graph topology and estimates the correlation matrix by leveraging an adaptive and graph topology oriented thresholding strategy. The additional topological information improves our Bayes factor thresholding decision by reducing false positive and false negative rates simultaneously. Simulation results demonstrate that our approach outperforms the competing thresholding and shrinkage methods. We also illustrate the application of our new method by analyzing of a serum mass spectrometry proteomics data set.

---

\*Correspondence to: shuochen@umd.edu

*Keywords:* graph, large correlation matrix, network, shrinkage, thresholding, topology.

# 1 Introduction

We consider a large data set  $\mathbf{X}_{n \times p}$  with the sample size  $n$  and the feature dimensionality of  $p$ . The estimation of the covariance matrix  $\mathbf{\Sigma}$  or correlation matrix  $\mathbf{R}$  is fundamental to understand the inter-relationship between variables of the large data set  $\mathbf{X}_{n \times p}$  (Fan *et al*, 2015).

When the dimensionality is high ( $p$  is large), the estimation by using sample covariance is known to have poor performance and regularization is required. Various regularization methods have been developed for this purpose. For instance,  $\ell_1$  penalized maximum likelihood have been utilized to estimate the sparse precision matrix  $\mathbf{\Theta} = \mathbf{\Sigma}^{-1}$  (Friedman *et al*, 2008; Banerjee *et al*, 2008; Yuan and Lin, 2007; Lam and Fan, 2009; Yuan, 2010; Cai and Liu, 2011; Shen *et al*, 2012). In addition, the covariance matrix thresholding methods have been developed to directly regularize the sample covariance matrix (Bickel and Levina, 08; Rothman *et al*, 2009; Cai *et al*, 2011; Zhang, 2010; Fan *et al*, 2013; Liu *et al*, 2014). Similarly, the thresholding regularization techniques have also been applied to correlation matrix  $\mathbf{R}$  estimation (Qi and Sun, 2006; Liu *et al*, 2014; Cui *et al*, 2016). Mazumder and Hastie (2012) and Witten *et al* (2011) point out that the two sets of methods are naturally linked regarding vertex-partition of the whole graph and estimate of the graph edge skeleton.

The regularization strategies including both covariance matrix thresholding and precision matrix shrinkage methods are often implemented on individual edges rather than considering the interactions between edges and the whole graph topology. Hence, a universal thresholding value or regularization standard is applied to to all edges without accounting for the dependency between edges. Cai and Liu (2011) propose adaptive thresholding methods by considering the variability of the individual entries, yet such thresholding strategy still applies the same decision rule to each entry independently without accounting for the whole graph topology.

Graph theory notations and definitions are often used to describe the relationship between the  $p$

variables of  $\mathbf{X}_{n \times p}$  (Yuan and Lin, 2007; Mazumder and Hastie, 2012). A finite undirected graph  $G = \{V, E\}$  consists two sets, where the vertex set  $V$  represents the variables  $\mathbf{X} = (X_1, \dots, X_p)$  with  $|V| = p$  and the edge set  $E$  denotes relationships between the vertices. Let  $e_{i,j}$  be the edge between nodes  $i$  and  $j$ . Then  $e_{i,j}$  is an connected edge if nodes  $i$  and  $j$  are genuinely correlated in  $G$ . Under the sparsity assumption, the regularization algorithms assign most edges as unconnected, and  $G$  may be decomposed to a set of maximal connected subgraphs (Witten *et al*, 2011; Mazumder and Hastie, 2012).

Previous studies show that the interactions between genes or neural processing units exhibit organized network graph topological properties (i.e. non Erdős-Rényi random graph). Recently, Cai *et al*, 2014 suggest the prior knowledge of the matrix structure may improve the regularization and estimation procedure. However, often the topological structure of covariance and precision matrices is latent and thus it is crucial to identify the topological patterns in a data-driven fashion for correlation matrix estimation. In this paper, we consider the scenario that there are latent community networks, and variables are more correlated with each other within each community network.

The latent community graph structure is naturally linked to the stochastic block model (SBM, Bickel and Chen, 2009; Karrer and Newman, 2011; Zhao *et al*, 2011; Choi *et al*, 2012; Nadakuditi and Newman, 2012; Lei and Rinaldo, 2014). However, the high-dimensional biomedical data tend to be different from the assumption of the SBM model because not all variables can be allocated to communities. Therefore, we consider a new model structure that  $G = G^1 \cup G^0$  where the subgraph  $G^1 = \cup_{c=1}^C G_c$  follows a SBM and  $G^0 = \cup_{m=1}^M G_m$  ( $G_m$  is a singleton only consisting one node) can be considered as an Erdős-Rényi random graph (i.e.  $G$  is a SBM-RG model). Thus, the SBM-RG model is a special case of SBM model and includes more singletons than general SBM model. Based on our observation, the practical massive biomedical data sets are more likely to follow a SBM-RG mixture model. From the perspective of clustering, the SBM-RG model categorizes many nodes into communities and the rest of nodes as singletons. We develop novel algorithms to implement the automatic detection of the latent SBM-RG model from an input (weighted) graph adjacency matrix without clear patterns. Our algorithms reflect the ‘rule of parsimony’ which ensures most variables in communities are highly correlated and minimize the number and sizes of communities

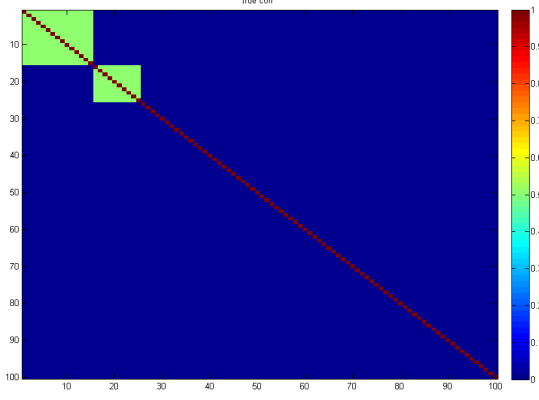
(i.e. to obtain ‘high quality’ communities). Our SBM-RG based community detection algorithm alone would contribute as a novel unsupervised learning technique for pattern recognition.

Our overarching goal is to estimate the network induced correlation matrix by adaptive thresholding, and the decision rule of thresholding is enlightened by the detected graph topological structure (i.e. the SBM-RG structure). Specifically, we perform adaptive thresholding for edges within and outside communities by using Bayes factors, and thus the regularization is guided by the graph topology as updated prior knowledge. In this way, the decision of thresholding an edge is made upon considering both this edge’s magnitude and the its location via the detected graph topological information. Therefore, our Bayes factor based adaptive thresholding strategy allows edges to borrow strength from each other without the tedious and impractical estimation of the covariance of edges (i.e. correlation of correlations). We name this new graph topology information guided regularization strategy **Network Induced Correlation matrix Estimation (NICE)**. NICE is distinct from the conventional graphical model based covariance/precision matrix estimation (e.g. glasso), because we first detect the non-random/organized graph topological patterns and then perform regularization by leveraging the topological patterns. We implement the NICE approach in two steps and we further provide theoretical results of the proposed algorithms.

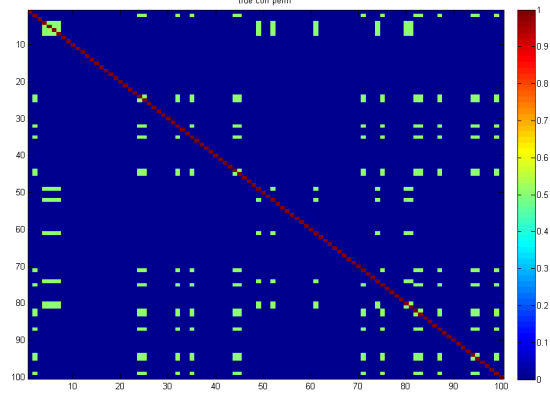
The paper is organized as follows. Section 2 describes the NICE algorithm, followed by theoretical results in Section 3. In Sections 4 and 5, we perform the simulation studies and model evaluation/comparison and we apply our method to the mass spectrometry proteomics data. Concluding remarks are summarized in Section 6.

## 2 Methods

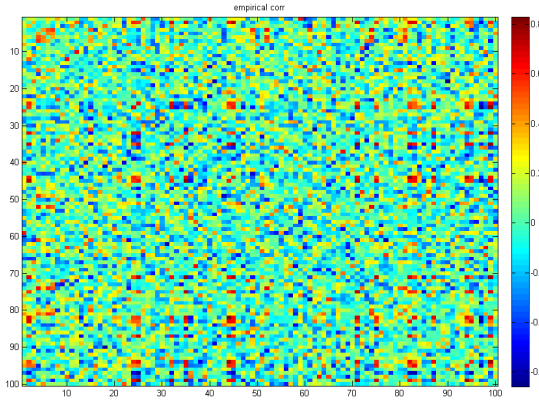
We consider the sample covariance  $\mathbf{S}$  and the sample correlation matrix  $\widehat{\mathbf{R}} = \text{diag}(\mathbf{S})^{-1/2} \mathbf{S} \text{diag}(\mathbf{S})^{-1/2}$  as our input data (Qi and Sun, 2006; Liu *et al*, 2014; Fan *et al*, 2015). We may directly perform thresholding/regularization on the sample correlation matrix to estimate  $\mathbf{R}$  by using  $R_{i,j}^T = \{\widehat{R}_{i,j} I(|\widehat{R}_{i,j}| > T)\}$ , where  $T$  is a pre-specified threshold. However, applying a universal regularization/thresholding rule (even when optimal  $T$  is provided) to each element (or column) may



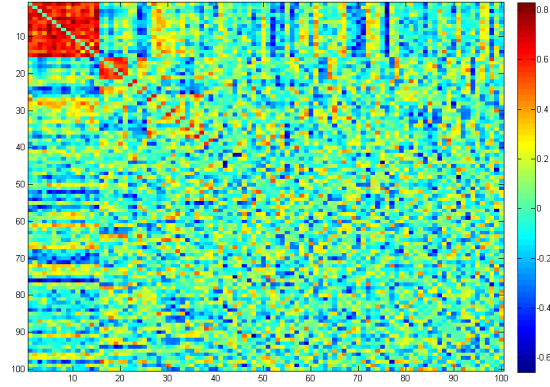
(a) The truth: two networks



(b) Shuffling the order of nodes



(c) The input data for NICE



(d) Network detection results

Figure 1: An example of a network induced covariance matrix:  $|V|=100$  nodes and  $|E|=4950$  edges, there are two networks (a) and in practice they are implicit (b) especially hard to recognize when looking at the sample covariance matrix (c); however, with the knowledge/estimation of topological network structures detected by NICE (d) the regularization strategy should take them into account.

introduce false positives and false negatives due to various noises from the sample data. Therefore, we seek to borrow information from the latent topological structure of the correlation matrix (i.e. graph  $G$ ) to assist our decision making process.

The NICE method consists two steps: i) detect the latent topological structure in the form of SBM-RG structure in  $G$  that  $G = G^1 \cup G^0 = (\cup_{k=1}^K G_c) \cup (\cup_{m=1}^M G_m)$  based on a (posterior probability) fuzzy logic metric weighted adjacency matrix  $\mathbf{W} = g(\hat{\mathbf{R}})$ ; ii) apply the adaptive thresholding rules guided by the detected graph topology.

## 2.1 Graph topological structure detection

### 2.1.1 Calculate posterior probability based fuzzy logic weight matrix $\mathbf{W}$

The input adjacency matrix is crucial for topological pattern recognition. We first propose a new method to calculate the weighted adjacency matrix from the input sample correlation matrix and ensure the metric of our new weighted adjacency matrix is well suited for the following topological pattern detection. Rather than directly thresholding/binarizing the sample correlation matrix  $\widehat{\mathbf{R}}$  by using  $\widehat{\delta}_{i,j} = I(|\widehat{R}_{i,j}| > T)$  (binary adjacency matrix), we calculate a fuzzy logic metric  $W_{i,j} = P(\delta_{i,j} = 1|\widehat{\mathbf{R}})$  by using an empirical Bayes framework (Chen *et al*, 2015a).  $\delta_{i,j}$  is a binary parameter indicating whether an edge should be thresholded. The fuzzy logic metric provides an appropriate scale for latent topological structure detection because it reflects the belief of an edge being connected by taking into the distribution of correlations on all edges. Let  $z_{i,j}$  be the Fisher's Z transformed correlation coefficient  $\widehat{R}_{i,j}$ , for instance (Kendall's Tau or other pairwise relationship metrics could also be applied). The sample correlation coefficient follows a mixture distribution  $z_{i,j} \sim \pi_0 f_0(z_{i,j}) + \pi_1 f_1(z_{i,j})$  where  $\pi_0 + \pi_1 = 1$ . The  $f_1$  represents the distribution of correlations corresponding to the component of connected edges  $z_{i,j} | (\delta_{i,j} = 0) \sim f_0(z_{i,j})$ , and  $f_0$  for the unconnected edges  $z_{i,j} | (\delta_{i,j} = 1) \sim f_1(z_{i,j})$ . We adopt the empirical Bayes method to obtain  $\hat{\pi}_0, \hat{\pi}_1, \hat{f}_0, \hat{f}_1$ , and we would refer the readers for the details to the original works (Efron, 2004; Wu *et al*, 2006; Efron, 2007). The Bayes posterior probability that a case belongs to the connected edge set given  $z_{i,j}$ , by definition, is:

$$\begin{aligned} E(W_{i,j}) &\equiv P\{\delta_{i,j} = 1|\widehat{\mathbf{R}}\} = \pi_1 f_1(z_{i,j}) / f(z_{i,j}) \\ &= (f(z_{i,j}) - \pi_1 f_1(z_{i,j})) / f(z_{i,j}) = 1 - \text{fdr}(z_{i,j}) \end{aligned} \tag{1}$$

In practice, we calculate the fuzzy logic metric  $W_{i,j} = 1 - \widehat{\text{fdr}}(z_{i,j})$  based on the estimated  $\text{fdr}$  by using the existing statistical package e.g. 'lcfdr' in the R software.

Therefore, the Bayes posterior probability based fuzzy logic metric provides a non-parametric trans-

formation to map the original correlation metric value of  $z_{i,j}$  to a probability based 0 to 1 scale (the probability of not be thresholded). The distribution of  $W_{i,j}$  often shows a large proportion of edges with the fuzzy logic values close to zero, and a small proportion greater than zero and close to one, which clearly improves the separation of signals from noises and greatly enhances the following graph topology structure detection. Thus, this transformation is a necessary step as it prominently improves the performance of network/topology structure detection based on numerous practical data analysis (von Luxburg, 2007).

Note that  $\mathbf{W}$  is calculated as the weighted adjacency matrix and does not directly involve with the regularization step. Let  $\delta_{i,j}$  be an indicator parameter of thresholding an edge and we consider it as a parameter of the Bayesian inferential framework (i.e. it follows a Bernoulli distribution). Contrastingly, in step two (estimating  $\mathbf{R}$  by adaptive thresholding) let  $\delta_{i,j}^0 \in \{0,1\}$  be the true parameter of interest indicating whether nodes  $i$  and  $j$  are connected or not, and estimate  $\delta_{i,j}^0$  by an adaptive thresholding procedure. The asymptotic properties are derived accordingly.

### 2.1.2 Detect the SBM-RG topological structure by using spectral graph methods

Next, we seek to detect the SBM-RG topology of  $G$  based on the input fuzzy logic metric weight matrix  $\mathbf{W}$ . Under the assumption that the  $G$  include induced complete subgraphs (community networks) as shown in 1a, the edges within the networks are more likely to be connected than edges outside networks. However, this topological structure is latent and the sample correlation matrix has no explicit network structure (1c). Thus, our goal is to automatically recognize such graph topological structures (from 1c to 1d).

One convenient pathway to reorder the nodes is to shuffle the nodes by allocating more correlated variables (nodes) to be adjacent to each other. However, the shuffling includes  $p!$  options (e.g.  $p! \doteq 10^{157}$  when  $p = 100$ ) and it is impractical to exhaust all permutations. Therefore, we need algorithms to implement this goal. For example, we may identify each network by cutting edges connecting the network with the rest of the graph. Then, it becomes an edge cutting problem.

Spectral clustering algorithms have been applied to optimize the edge cutting problem for example

using Ratio-Cut and Normalized Cut algorithms (von Luxburg, 2007; Nadakuditi and Newman, 2012). Given an appropriate number of clusters  $C$ , the spectral clustering methods provide a promising solution to cut edges and detect networks. However, different from the traditional goal of spectral clustering that allocates all nodes into  $C$  classes, we try to detect a graph  $G$  that not only includes many community networks ( $G^1 = \cup_{c=1}^C G_c$ ) and the rest of  $G$  can be considered as an Erdős-Rényi random graph ( $G^0$ ). To detect such graph topological structure, we not only need to cut the edges between communities in  $G^1$  but also most edges in  $G^0$  and between  $G^0$  and  $G^1$ . To cut edges of  $G$  with the above topological structure, the Normalized Cut algorithm seems not well suited because it may allocate the networks with similar sizes and fail to detect singletons in  $G^0$  the Erdős-Rényi random graph. We propose the objective function based on the RatioCut algorithm. The edge cutting objective function is to minimize:

$$\operatorname{argmin}_{\{G_c\}_{c=1}^C} \sum_{c=1}^C \frac{\sum_{i \in G_c, j \notin G_c} W_{i,j}}{|V_c|}, \quad (2)$$

It minimizes the fuzzy logic metric values ( $W_{i,j}$ ) of the edges between networks (including network of size one). The denominator  $|V_c|$  prevents to generate with one major community and  $C - 1$  singletons. Thus, the objective function lead to cutting those between network edges whose sum of fuzzy logic metric values is minimum. The network detection and edge cutting are obtained simultaneously when implementing minimization of 2. It is NP complex to implement the optimization of 2, and fortunately computational algorithms have been successfully developed for solutions (Shi and Malik, 2000; Chen *et al*, 2015b). It has been established (Chung, 1997) that the 1 is equivalent to

$$\operatorname{argmin} \sum_{c=1}^C \mathbf{h}_i \mathbf{L} \mathbf{h}_i = \operatorname{Tr}(\mathbf{H}' \mathbf{L} \mathbf{H}), \quad (3)$$

where  $\mathbf{H}_{p \times C}$  is indicator matrix and a column  $h_k$  of  $\mathbf{H}$  is a binary  $p \times 1$  vector (elements with entry value 1 indicate that they belong to the  $c$ th network). Estimating  $\mathbf{H}_{p \times C}$  provides the network detection results.  $\mathbf{L}$  is the Laplacian matrix, which is defined by:



$$\mathbf{L} = \mathbf{D} - \mathbf{W}, \quad (4)$$

where  $\mathbf{D} = \text{diag}(\sum_j^p W_{i,j})$  and  $i = 1, \dots, p$ . We implement the optimization of 4 to estimate  $\mathbf{H}_{p \times K}$  by using unnormalized graph Laplacian (von Luxburg, 2007) and details are provided in the Algorithm 1. Furthermore, Lei and Rinaldo (2014) provides proof of consistency with regard to spectral clustering for SBM. Therefore,  $\hat{G}$  provides a satisfactory estimation of topological structure of  $G$  when  $C$  is appropriately selected, and both communities  $G^1$  and singletons  $G^0$  can be detected.

### 2.1.3 Select the optimal $C$ objectively: the ‘quantity and quality’ criterion

It is crucial to select an appropriate number of  $C$ , because it not only influences the community detection (allocation of nodes) but also the proportions of  $G^0$  and  $G^1$ . For example, if  $C = |V|$  then all edges will be cut in  $G$  (then  $G$  is an Erdős-Rényi random graph) while if  $C=1$  then no edge will be cut. Thus, the selection of  $C$  determines the estimation of the graph topological structure of  $G$ , and then it further influences the following graph topology oriented regularization. However, the most commonly used  $C$  selection methods in spectral clustering such as eigengap heuristic, stability approach, and information-theoretic criteria are not well suited for detecting the SBM-RG structure because often these methods yield a relatively small value of  $C$  which may lead to the failure of  $G^0$  (singletons) identification (von Luxburg, 2007). The smaller value of  $C$  may also include a higher proportion of low-correlation edges into communities as noises and misguide the following regularization step.

We propose a novel ‘quantity and quality’  $C$  selection procedure. Our heuristic to choose the  $C$  that maximizes the number of highly correlated edges ( $W_{i,j}$  with larger values) inside community networks (the ‘quantity’ criterion) when ensuring that the detected community networks have a high proportion of informative edges (the ‘quality’ criterion). We implement the ‘quantity and quality’ criterion by maximizing:

$$\frac{\sum_{c=1}^C \sum_{i \in G_c, j \in G_c} W_{i,j}}{\sum_{i < j} W_{i,j}} \cdot \frac{\sum_{c=1}^C \sum_{i \in G_c, j \in G_c} W_{i,j}}{\sum_{c=1}^C \sum_{i \in G_c, j \in G_c} 1}. \quad (5)$$

The first term (the ratio of informative edges included in the network with contrast to the informative edges in the whole graph) reflects the ‘quantity criterion’ and the second term for the ‘quality criterion’ (the ratio of informative edges in the networks with contrast to the total number of edges in those networks). The ‘quantity’ criterion tries to include most informative edges into the detected community networks  $G_c$ , whereas the ‘quality’ criterion ensures most edges in the detected networks are highly correlated. We consider  $W_{i,j}$  with larger values as informative edges because generally  $P(\delta_{i,j} = 1) > P(\delta_{i',j'} = 1)$  if  $W_{i,j} > W_{i',j'}$  without considering other information. In practice, if the dimension  $p$  is high we replace  $W_{i,j}$  in 5 by  $I(W_{i,j} > p_0)$  (e.g.  $q_0 = 0.10$ ) to avoid the accumulation of false positive noises. This procedure generally has little influence as most  $W_{i,j}$  values are zeros (dominated by the null component). We optimize 5 by grid searching because  $C$  can only be integers from two to  $p$ . The NICE algorithm selects  $C$  objectively, and the SBM-RG topology detection algorithm is data-driven.

By applying spectral clustering algorithm and optimizing  $C$  using the ‘quantity and quality’ criterion, the NICE algorithm produces the result of  $\cup_{c=1}^C G_c = G$  (where many  $G_c$  are singletons). Note that  $G_c$  is a community network if and only if i) the number of nodes  $\hat{V}_c \geq 3$  and ii) the proportion of informative edges is significantly higher than the null that all informative edges are randomly distributed. We verify the condition (ii) by using permutation tests (see details in the algorithm table). The heuristic of permutation test follows: if graph  $G$  has a latent and organized topological structure (i.e. SBM-RG model holds), the uncovered community networks include higher proportion of correlated edges within the detected network and  $\sum_{i,j \in G_c} W_{i,j}$  is larger than the sum of whole graph average level. Under the null hypothesis that  $G$  is a random graph, the probability of observe most informative edges in constrained subgraphs is extremely low based on the graph combinatorics. The final products of the graph topology detection of  $G$  are 1) the  $\cup_{c=1}^C G_c$  and permutation test based significant community networks and 2) a label of each edge indicating whether this edge is located inside a community network. Therefore, we generally consider there are two types of edges:

inside-network edges and outside-network edges. If the SBM-RG topological structure exists (we can also test this assumption by permutation tests), the in-network edges have stronger correlation values than outside-network edges. The graph topology may become prior knowledge to improve the regularization  $\widehat{\delta}_{i,j}$  and reduce false positive and false negative rates simultaneously.

## 2.2 Graph topology oriented adaptive correlation matrix thresholding

To estimate the correlation matrix  $\mathbf{R}$ , we perform graph topology guided adaptive thresholding on the sample correlation matrix  $\widehat{\mathbf{R}}$  by using Bayes factors. Let  $z_{i,j}$  be the Fisher's Z transformed sample correlation coefficient of  $\widehat{R}_{i,j}$  and  $z_{i,j} \sim \pi_0 f_0(z_{i,j}) + \pi_1 f_1(z_{i,j})$ .

### *Universal thresholding*

Without prior information of topology structure, we perform universal thresholding on individual edges. We select the threshold by using Bayes factor via the empirical Bayes framework (Efron, 2007, Schäfer and Strimmer, 2005). The decision rule is that the hard-thresholding sets an edge to zero unless

$$\frac{P(\delta_{i,j} = 1 | z_{i,j})}{P(\delta_{i,j} = 0 | z_{i,j})} = \frac{f_1(z_{i,j})\pi_1}{f_0(z_{i,j})\pi_0} \geq T, \quad (6)$$

where  $T$  is a constant that is linked to local  $fdr$  cutoff, and  $\pi_0$  and  $\pi_1$  are the proportions of null and non-null distributions correspondingly. For example,  $T = 4$  is equivalent to the cutoff of local  $fdr$  of 0.2 (Efron, 2007). For instance, given  $\pi_0 = 0.9$  and  $\pi_1 = 0.1$ , the universal decision rule is that an edge is thresholded when  $BF = \frac{f_1(z_{i,j})}{f_0(z_{i,j})} \leq 36$ . In practice,  $\pi_0$  and  $\pi_1$  are estimated based on the distribution of the statistics (e.g.  $z_{i,j}$ ) and the Bayes factor cut-off is updated accordingly.

It has been well documented that the Bayes factor inferential models could adjust the multiplicity by adjusting the prior structure (Jeffreys, 1961; Kass and Raftery, 1995; Scott and Berger, 2006; Efron, 2007; Scott and Berger, 2010). The prior odds are tuned to control false positive rates, and a larger  $\pi_0$  ( $\pi_0 \rightarrow 1$ ) or a distribution of  $\pi_0$  with larger mean leads to more stringent adjustment that may cause both low false positive discovery rates and high false negative discovery rates. Scott

and Berger, 2006 suggest a prior distribution with median value around 0.9 and Efron, 2007 estimates  $\pi_0$  by using an empirical Bayes model. These methods are developed for the node based (e.g. gene expression or brain activation analysis) inference, and may not directly applicable to correlation matrix thresholding for edge level inference. The universal regularization (shrinkage or thresholding) has been facing the trade-off between false positive and false negative findings and one possible remedy is adaptive thresholding. Furthermore, edges may be dependent on each other in an organized topological pattern and the mass univariate edge inference (universal regularization) ignoring the dependency structure may not control false positive and negative rates efficiently. However, the direct estimation of the dependency structure between edges is challenging and sometime not feasible. The prior knowledge of detected topological structure provides precise neighborhood information that allows edges to borrow strength for each other, and thus we can account for the dependency between edges leveraging the topological structure. Specifically, we adopt the adaptive Bayes factor thresholding by updating prior knowledge of  $\pi_0$  and  $\pi_1$  for each edge  $e_{i,j}$  based on the detected topological structure (i.e.  $e_{i,j}$  belongs to inside or outside networks of a SBM-RG graph).

#### *Graph topology oriented adaptive thresholding*

In a network induced correlation matrix, the variables in the community networks are more correlated and thus the edges are very likely to be connected. We update the prior odds for edges within and outside community networks separately by:

$$\frac{P(\delta_{i,j} = 0 | e_{i,j} \in G_c, \forall c)}{P(\delta_{i,j} = 1 | e_{i,j} \in G_c, \forall c)} = \frac{\pi_0^{in}}{\pi_1^{in}} = \theta_{in}, \text{ and } \frac{P(\delta_{i,j} = 0 | e_{i,j} \notin G_c, \forall c)}{P(\delta_{i,j} = 1 | e_{i,j} \notin G_c, \forall c)} = \frac{\pi_0^{out}}{\pi_1^{out}} = \theta_{out} \quad (7)$$

where  $\theta_{out} \geq \theta_{all} \geq \theta_{in}$ . We let edges inside and outside of the detected communities follow different distributions:  $z_{i,j} | e_{i,j} \in G_c \sim \pi_0^{in} f_0(z_{i,j}) + \pi_1^{in} f_1(z_{i,j})$  and  $z_{i,j} | e_{i,j} \notin G_c \sim \pi_0^{out} f_0(z_{i,j}) + \pi_1^{out} f_1(z_{i,j})$ . We assume that the null  $f_0(z_{i,j})$  and non-null  $f_1(z_{i,j})$  distributions are identical, but the proportions are different for inside, outside and overall edges.

In step one, we have identified the latent community networks where edges are more correlated.

Thus, we propose the graph topology (i.e. SBM-RG structure) oriented adaptive thresholding rule:

If  $e_{i,j} \in G_c$ ,

$$\widehat{R}_{i,j}^{\mathcal{T}} = \begin{cases} \widehat{R}_{i,j} & \text{if } BF_{i,j} = \frac{\widehat{f}_1(z_{i,j})}{\widehat{f}_0(z_{i,j})} \geq T \cdot \widehat{\theta}_{in}; \\ 0 & \text{otherwise.} \end{cases}$$

else if  $e_{i,j} \notin G_c$ ,

$$\widehat{R}_{i,j}^{\mathcal{T}} = \begin{cases} \widehat{R}_{i,j} & \text{if } BF_{i,j} = \frac{\widehat{f}_1(z_{i,j})}{\widehat{f}_0(z_{i,j})} \geq T \cdot \widehat{\theta}_{out}; \\ 0 & \text{otherwise.} \end{cases}$$

Equivalently, the we provide estimate of the edge set  $\widehat{E}$  by using:

$$\begin{aligned} \widehat{\delta}_{i,j}^{in} &= I \left( \frac{\widehat{f}_1(z_{i,j})}{\widehat{f}_0(z_{i,j})} \geq T \cdot \widehat{\theta}_{in} \right); \\ \widehat{\delta}_{i,j}^{out} &= I \left( \frac{\widehat{f}_1(z_{i,j})}{\widehat{f}_0(z_{i,j})} \geq T \cdot \widehat{\theta}_{out} \right). \end{aligned} \tag{8}$$

The detected graph topology provides the prior knowledge of the ‘neighborhood’ and ‘location’ of an edge which accordingly updates the priors of the Bayes factor thresholding. A community network is analogous to a neighborhood (spatial closeness) of *edges* with explicit boundaries and the edges within the neighborhood could borrow power from each other. Many statistical models are developed based on this idea, for example, the Ising prior and conditional autoregressive (CAR) model (Besag and Kooperberg, 1995). Nevertheless, unlike spatial or imaging statistics the original correlation/covariance matrix of large biomedical data sets often include no available information about spatial location or closeness. Thus, our approach provides a new pathway of regularization/statistical inferences on ‘edges’ by accounting for the dependency structure based on detected graph topological ‘closeness’ via an empirical Bayes framework.

In practice,  $\widehat{\theta}_{in}$  and  $\widehat{\theta}_{out}$  are directly estimated from the data. First, all edges are Fisher’s Z transformed correlation coefficients in  $\widehat{\mathbf{R}}$  that follow a mixture distribution  $f(z_{i,j}) = \pi_0^{all} f_0(z_{i,j}) + \pi_1^{all} f_1(z_{i,j})$ , and  $\widehat{\pi}_0^{all}, \widehat{\pi}_1^{all}, \widehat{f}_0, \widehat{f}_1$  are estimated in step one. Next, we estimate  $\widehat{\pi}_0^{in}$  for in-network

edges  $e_{i,j} \in G_c$ . Since  $\hat{f}_0, \hat{f}_1$  are estimated in step one, the only parameter to estimate in  $f^{in}(z_{i,j}) = \pi_0^{in} f_0(z_{i,j}) + \pi_1^{in} f_1(z_{i,j})$  is  $\hat{\pi}_0^{in} = 1 - \hat{\pi}_1^{in}$ . We simply implement the estimation by using maximum likelihood estimation (MLE) and then calculate  $\hat{\theta}_{in} = \hat{\pi}_0^{in} / \hat{\pi}_1^{in}$ . Similarly, for edges outside of networks ( $z_{i,j}$  that  $e_{i,j} \notin G_c$ )  $f^{out}(z_{i,j}) = \pi_0^{out} f_0(z_{i,j}) + \pi_1^{out} f_1(z_{i,j})$  we estimate  $\hat{\pi}_0^{out}$  by MLE and calculate  $\hat{\theta}_{out} = \hat{\pi}_0^{out} / \hat{\pi}_1^{out}$ . In general, our graph topological structure detection algorithm produces a very small odds ratio  $\hat{\theta}^{in} / \hat{\theta}^{out}$  when the informative edges are distributed in an organized pattern. The small odds ratio  $\hat{\theta}^{in} / \hat{\theta}^{out}$  is guaranteed by [2](#) and [5](#).

#### *A convenient formula for graph topology oriented thresholding cut-off calculation*

As demonstrated above, our graph topology guided thresholding is closely related to calculation of local  $fdr$ . We derive a convenient formula to implement our graph topology oriented thresholding cut-off. In step one, a local  $fdr$  value is calculated for each edge that is  $1 - W_{i,j}$ . For  $e_{i,j} \in G_c$ , we threshold an edge if

$$1 - W_{i,j} \leq \frac{1}{T \hat{\theta}_{in} / \hat{\theta}_{all} + 1}.$$

For  $e_{i,j} \notin G_c$ , we threshold an edge if

$$1 - W_{i,j} \leq \frac{1}{T \hat{\theta}_{out} / \hat{\theta}_{all} + 1}.$$

We pre-specify value of  $fdr$  and  $T = (1 - fdr) / fdr$ , for example  $fdr = 0.2$  and  $T = 4$ . Although the thresholds are different for edges inside and outside the networks, given each edge's ‘neighborhood’ information based on the detected topological structure we control the local  $fdr$  at the same rate  $1/T + 1$  (see details in Appendix). Since in general  $\hat{\theta}_{out} \geq \hat{\theta}_{all} \geq \hat{\theta}_{in}$ , numerically we apply a stringent threshold for edges outside the community networks and a loose threshold for edges inside the community networks. The difference of thresholding values are determined by the difference between distributions of  $z_{i,j}^{in}$  and  $z_{i,j}^{out}$ . If no topological patterns can be captured, our graph topology oriented adaptive thresholding boils down to the universal thresholding by [Shäfer and Strimmer, 2005](#).

*Remarks:* the statistical inferences on large covariance/correlation matrices are challenging because edges are dependent on each other and dependent structure is often latent and complex yet possibly organized. Uncovering the graph topological structure is fundamental to understanding the interactive relationships between multivariate variables (nodes) and between edges. In turns, the detected topological structure becomes prior knowledge to improve topological structure assisted large covariance/correlation matrix regularization and estimation. We summarize the NICE algorithm of both steps in Algorithm 1.

---

**Algorithm 1** NICE algorithm

---

- 1: **procedure** NICE-ALGORITHM
  - 2:     Obtain the empirical Bayes fuzzy logic matrix  $\mathbf{W} = g(\hat{\mathbf{R}})$ ;
  - 3:     Calculate the Laplacian matrix  $\mathbf{L} = \mathbf{D} - \mathbf{W}$
  - 4:     **for** cluster number  $C = 2 : |V| - 1$  **do**
  - 5:         Compute the first  $C$  eigenvectors  $[u_2, \dots, u_C]$  of  $L$ , with eigenvalues ranked from the smallest;
  - 6:         Let  $U = [u_2^T, \dots, u_C^T]$  be a  $|V| \times C$  matrix containing all  $C - 1$  eigenvectors;
  - 7:         Perform K-means clustering algorithm on  $U$  with number of clusters of  $C$  to cluster  $|V|$  nodes into  $C$  networks;
  - 8:         Calculate the ‘quality and quantity’ criterion for each  $C$ .
  - 9:     **end for**
  - 10:     Adopt the clustering results using the  $C$  of the maximum score of the ‘quality and quantity’ criterion.
  - 11:     Identify the networks with significantly high proportion of correlated edges by using permutation test: for each detected community network  $G_c$  in  $G$ 
    - i) calculate the  $T_c^0 = -\log(1 - \frac{1}{\Gamma(|E_c|)}\gamma(|E_c|, \sum_{i,j \in G_c} -\log(W_{i,j})))$ , where  $\Gamma$  is the upper incomplete gamma function and  $\gamma$  is the lower incomplete gamma function;
    - ii) list all  $\{W_{i,j}\}$  in  $\mathbf{W}$  as a vector and shuffle the order of the vector and assemble the shuffled vector as a permuted  $\mathbf{W}^m$  for  $M$  (e.g. 10,000) times;
    - iii) calculate the maximum statistic  $T_{max}^m$  for all detected communities in each iteration;
    - iv) calculate the percentile of  $T_c^0$  in  $\{T_{max}^m\}$ , if it is less than the  $\alpha$  level then the network  $G_c$  is considered as a true community network.
  - 12:     Implement the topological structure oriented thresholding strategies for covariance entries inside and outside networks (see details in 2.2)
  - 13: **end procedure**
-

### 3 Theoretical Results

We start with some notations for the theoretical development. Let  $X_{i,k}$  be the observed data on node  $i$  for subject  $k$ , for  $i = 1, \dots, p_n$  and  $k = 1, \dots, n$  with mean zero and unit standard deviation. Recall that  $\mathbf{R} = \{R_{i,j}\}$  is the true correlation matrix of interests with  $\text{Cor}(X_{i,k}, X_{j,k}) = R_{i,j}$  and  $\hat{\mathbf{R}} = \{\hat{R}_{i,j}\}$  be the correlation matrix estimator. Let  $\text{Fis}(x) = \log\{(1+x)/(1-x)\}/2$  be the Fisher's Z transformation. Let  $z_{i,j} = \text{Fis}(\hat{R}_{i,j})$  and  $\mu_{i,j} = \text{Fis}(R_{i,j})$ . Note that we have  $R_{i,j} = 0$  if and only if  $\mu_{i,j} = 0$ . Let  $f_{i,j}(\cdot)$  be the density function of  $z_{i,j}$ . Let  $\phi(x) = \exp(-x^2/2)/\sqrt{2\pi}$  be the standard normal probability density function. Let  $\delta_{i,j}^0 = I[R_{i,j} \neq 0] = I[\mu_{i,j} \neq 0] = I[e_{i,j} \in G]$  indicate whether or not  $e_{i,j} \in G$ . Let  $q_n = \sum_{1 \leq i < j \leq p_n} \delta_{i,j}^0$ ,

$$f_0(z) = \frac{\sum_{i < j} (1 - \delta_{i,j}^0) f_{i,j}(z)}{\sum_{i < j} (1 - \delta_{i,j}^0)}, \quad \text{and} \quad f_1(z) = \frac{\sum_{i < j} \delta_{i,j}^0 f_{i,j}(z)}{\sum_{i < j} \delta_{i,j}^0}.$$

Let  $f(z)$  denote the actual distribution of  $\{z_{i,j}\}_{1 \leq i < j \leq p_n}$ .

$$f(z) = \pi_0 f_0(z) + \pi_1 f_1(z),$$

where

$$\pi_0 = \frac{p_n(p_n - 1) - q_n}{p_n(p_n - 1)} \quad \text{and} \quad \pi_1 = 1 - \pi_0.$$

Given data  $\{z_{i,j}\}_{i < j}$ , suppose  $\hat{f}_k(\cdot)$  be an estimator for  $f_k(\cdot)$  for  $k = 0, 1$ , and  $\hat{\pi}_0$  is an estimator for  $\pi_0$  with  $\hat{\pi}_1 = 1 - \hat{\pi}_0$ . For any  $T > 0$  and  $\hat{\mathbf{R}}$ , define the NICE thresholding operator  $\text{NICE}(\hat{\mathbf{R}}; T) = \{\text{NICE}(\hat{R}_{i,j}; T)\}_{i < j}$ . Specifically,

$$\text{NICE}(\hat{R}_{i,j}; T) = \begin{cases} \hat{R}_{i,j}, & \frac{\hat{f}_1(z_{i,j})}{\hat{f}_0(z_{i,j})} > \frac{\hat{\pi}_0}{\hat{\pi}_1} T, \\ 0 & \frac{\hat{f}_1(z_{i,j})}{\hat{f}_0(z_{i,j})} \leq \frac{\hat{\pi}_0}{\hat{\pi}_1} T. \end{cases}$$



### 3.1 Conditions

The following conditions are needed to facilitate the technical details, although they may not be the weakest conditions.

**Condition 3.1.** *We consider the following conditions on the data  $\mathbf{X} = (X_{i,k})$ .*

1. *Data are centered around zero with unit variance. i.e  $E[X_{i,k}] = 0$  and  $\text{Var}[X_{i,k}] = 1$ .*

2. *Data are uniformly bounded. That is, there exists a constant  $M > 0$  such that*

$$P[|X_{i,k}| < M] = 1,$$

3. *The Pearson's correlation estimator is computed by*

$$\widehat{R}_{i,j} = \frac{1}{n} \sum_{k=1}^n X_{i,k} X_{j,k},$$

4. *The population level correlation satisfy*

$$|R_{i,j}| = |E[X_{i,k} X_{j,k}]| < 1.$$

*for all  $1 \leq i, j \leq p_n$  and  $k = 1, \dots, n$ .*

**Condition 3.2.** *There exist constants  $c_0 > 0$  and  $\tau > 0$ , such that*

$$\mu_{\inf} = \inf_{i < j} \{|\mu_{i,j}| : \delta_{i,j}^0 = 1\} = c_0 n^{-1/2+\tau}.$$

**Condition 3.3.** *Let  $\tau > 0$  be the same constant in Condition 3.2. Then*

$$\log(p_n) = o(n^{2\tau}).$$

**Condition 3.4.** Suppose there exists  $0.5 < \pi_0 < 1$ , such that

$$\lim_{n \rightarrow \infty} \pi_0 = \pi_0 \text{ and } \lim_{n \rightarrow \infty} \pi_1 = 1 - \pi_0.$$

**Condition 3.5.** Given data  $\{z_{i,j}\}_{i < j}$ , suppose  $\hat{f}_k(\cdot)$  be a consistent estimate for  $f_k(\cdot)$  for  $k = 0, 1$ . Suppose  $\hat{\pi}_0$  is consistent estimates for  $\pi_0$ . Specifically, for any  $\epsilon > 0$ ,

$$\lim_{p_n \rightarrow \infty} \mathbb{P}\{\|\hat{f}_k(\cdot) - f_k(\cdot)\|_2 + |\hat{\pi}_0 - \pi_0| > \epsilon\} = 0.$$

where  $\|\cdot\|_2$  be the  $L_2$  norm for the function, which is defined as  $\|f\|_2 = \int_{\mathbb{R}} \{f(x)\}^2 dx$ .

**Condition 3.6.** Let  $\omega$  be the proportion of edges inside community networks and  $\int_{z_0}^{\infty} f(z_{i,j}) = F(z_0)$ .

$$\frac{F_0(z_0) - F_0(z_{out})}{F_0(z_{in}) - F_0(z_0)} > \frac{\omega \pi_0^{in}}{(1 - \omega) \pi_0^{out}}$$

**Condition 3.7.** Let  $\omega$  be the proportion of edges inside community networks and  $\int_{z_0}^{\infty} f(z_{i,j}) = F(z_0)$ .

$$\frac{F_1(z_0) - F_1(z_{out})}{F_1(z_{in}) - F_1(z_0)} < \frac{\omega \pi_1^{in}}{(1 - \omega) \pi_1^{out}}$$

## 3.2 Tail Probability Bounds

By Berry-Esseen theorem and Taylor expansion, it is straightforward to show the following lemma:

LEMMA 3.1. For any  $i < j$ ,

$$\lim_{n \rightarrow \infty} \sup_{z \in \mathbb{R}} |f_{i,j}(z) - \sqrt{n} \phi\{\sqrt{n}(z - \mu_{i,j})\}| = 0.$$

In addition, we also need to study the probability bound of the  $z_{i,j}$ . Specifically, we have the following lemma:

LEMMA 3.2. Suppose Condition 3.1 holds. For all  $1 \leq i, j \leq p_n$ , there exists a constant  $K > 0$  and

$N > 0$ , for and  $n > N$ , and any  $\epsilon > 0$ , we have

$$P[\sqrt{n}|z_{i,j} - E[z_{i,j}]| > \epsilon] \leq \exp(-K\epsilon^2).$$

By Lemma 3.1 and Condition 3.1, we can uniformly approximate  $f_1(z)/f_0(z)$ , which is stated in the following lemma:

LEMMA 3.3.

$$\begin{aligned} \lim_{n \rightarrow \infty} \sup_{z \in \mathbb{R}} |f_0(z) - \sqrt{n}\phi\{\sqrt{n}z\}| &= 0, \\ \lim_{n \rightarrow \infty} \sup_{z \in \mathbb{R}} \left| f_1(z) - \frac{1}{q_n} \sum_{i < j} \delta_{i,j}^0 \sqrt{n}\phi\{\sqrt{n}(z - \mu_{i,j})\} \right| &= 0, \end{aligned}$$

and

$$\lim_{n \rightarrow \infty} \sup_{z \in \mathbb{R}} \left| \frac{f_1(z)}{f_0(z)} - \frac{\pi_0}{\pi_1} \frac{\sum_{i < j} \delta_{i,j}^0 \phi\{\sqrt{n}(z - \mu_{i,j})\}}{(p_n(p_n - 1)/2 - q_n)\phi(\sqrt{n}z)} \right| = 0,$$

LEMMA 3.4. Suppose Conditions 3.2–3.4 hold. There exist constants  $C_0 > 0$  and  $C_1 > 0$  such that for any  $i < j$  and any  $T > (1 - \pi_0)/\pi_0$ , there exists  $N_T > 0$ , for all  $n > N_T$ , we have when  $e_{i,j} \in G$ , then

$$P \left[ \frac{\sum_{i' < j'} \delta_{i',j'}^0 \phi\{\sqrt{n}(z_{i,j} - \mu_{i',j'})\}}{\{p_n(p_n - 1)/2 - q_n\}\phi(\sqrt{n}z_{i,j})} \leq T \right] \leq \exp(-C_1 n^{2\tau}).$$

And when  $e_{i,j} \notin G$ , then

$$P \left[ \frac{\sum_{i',j'} \delta_{i',j'}^0 \phi\{\sqrt{n}(z_{i,j} - \mu_{i',j'})\}}{\{p_n(p_n - 1)/2 - q_n\}\phi(\sqrt{n}z_{i,j})} > T \right] \leq C_2 \exp(-C_0 n^{2\tau}).$$

Note that  $N_T$  depends on  $T$  but it does not depend on  $i$  and  $j$ .

### 3.3 Selection and Estimation Consistency

We construct the population level selection indicator  $\tilde{\delta}_{i,j}(T)$  and the selection indicator estimator  $\hat{\delta}_{i,j}(T)$  and discuss their properties in Lemmas 3.5 and 3.6 respectively.

LEMMA 3.5. Suppose Conditions 3.2–3.4 hold. For all  $i < j$  and any  $T > (1 - \pi_0)/\pi_0$ , let

$$\tilde{\delta}_{i,j}(T) = I \left[ \frac{\pi_1 f_1(z_{i,j})}{\pi_0 f_0(z_{i,j})} > T \right].$$

Then there exist  $N_T > 0$ ,  $C_3 > 0$  and  $C_4 > 0$  such that for any  $n > N_T$ ,

$$P\{\tilde{\delta}_{i,j}(T) \neq \delta_{i,j}^0\} \leq C_3 \exp(-C_4 n^{2\tau}).$$

where  $N_T$  depends on  $T$  but not on  $i$  and  $j$ , and  $\tau > 0$  is the same constant in Condition 3.2.

LEMMA 3.6. For any  $T > (1 - \pi_0)/\pi_0$  and any  $i < j$ , let

$$\hat{\delta}_{i,j}(T) = I \left[ \frac{\hat{\pi}_1 \hat{f}_1(z_{i,j})}{\hat{\pi}_0 \hat{f}_0(z_{i,j})} > T \right].$$

Then there exists  $N_T > 0$  such that for all  $n > N_T$ ,

$$P[\hat{\delta}_{i,j}(T) \neq \delta_{i,j}^0] \leq C_3 \exp(-C_4 n^{2\tau}),$$

where the constants  $C_3$ ,  $C_4$  and  $\tau$  are the same as the ones in Lemma 3.5.

We establish the selection consistency and estimation consistency in the following two theorems respectively.

THEOREM 1. (Selection Consistency) Suppose Conditions 3.1 – 3.5 hold. Denote by  $\Delta_0 = \{\delta_{i,j}^0\}_{i < j}$  all the edge indicators. For any  $T > (1 - \pi_0)/\pi_0$ , let  $\hat{\Delta}(T) = \{\hat{\delta}_{i,j}(T)\}_{i < j}$ , then there exists  $N_T > 0$  for all  $n > N_T$ ,

$$P\{\hat{\Delta}(T) = \Delta_0\} \geq 1 - \frac{C_3}{2} p_n(p_n - 1) \exp(-C_4 n^{2\tau}).$$

where the constants  $C_3$ ,  $C_4$  and  $\tau$  are the same as the ones in Lemma 3.5. Furthermore,

$$\lim_{n \rightarrow \infty} P\{\hat{\Delta}(T) = \Delta_0\} = 1.$$

THEOREM 2. (Estimation Consistency) Suppose Conditions 3.1 – 3.5 hold and the constant  $\tau$  in

Condition 3.5 satisfies  $0 < \tau < 1/2$ . For any  $\epsilon > 0$  and any  $T > (1 - \pi_0)/\pi_0$ , we have

$$\lim_{n \rightarrow \infty} \mathbb{P}[\|\text{NICE}(\widehat{\mathbf{R}}; T) - \mathbf{R}\|_\infty > \epsilon] = 0,$$

where  $\|\mathbf{M}\|_\infty$  is the  $L^\infty$  norm, i.e.  $\|\mathbf{M}\|_\infty = \max_{1 \leq i, j \leq p_n} |m_{i,j}|$  for any matrix  $\mathbf{M} = (m_{i,j})$ .

### 3.4 Superiority of false positive and negative rates by using graph topology oriented adaptive thresholding

**THEOREM 3.** (*Expected false positive and negative edges*) Suppose Conditions 3.6 and 3.7 hold, we have both

i)  $E^A(\#FP) < E^U(\#FP)$ : the expected false positively thresholded edges of our graph topology oriented thresholding ( $E^A(\#FP)$ ) are less than the universal thresholding ( $E^U(\#FP)$ ).

ii)  $E^A(\#FN) < E^U(\#FN)$ : the expected false negatively thresholded edges of our graph topology oriented thresholding ( $E^A(\#FN)$ ) are less than the universal thresholding ( $E^U(\#FN)$ ).

## 4 Simulation Studies

We conduct numerical studies to evaluate the performance of our approach, and compare it with several existing popular methods.

### 4.1 Synthetic data sets

We simulate each data set with  $p = 100$  variables, and thus  $|V| = 100$  and  $|E| = \binom{100}{2} = 4950$ . We assume that the correlation matrix includes two community networks, and the first include 15 nodes and the second 10 nodes. The induced networks are complete subgraphs (cliques) that all edges are connected within these two networks and no other edges are connected outside the two networks (Fig 1a). Next, we permute the order of the nodes to mimic the practical data where the

topological structure is latent. (Fig 1b) represents the correlated edges in the matrix. Let vector  $\mathbf{x}_{p \times 1}^k$  follow a multivariate normal distribution, with zero mean and covariance matrix  $\Sigma_{p \times p}$ , and the sample size is  $n$ .  $\sigma_{i,j}$  is an entry at the  $i$ th row and  $j$ th column of  $\Sigma$ ,  $\sigma_{i,j} = 1$  if  $i = j$  (then  $\Sigma = \mathbf{R}$ ), and  $\sigma_{i,j} = \rho$  if  $e_{i,j} \in G_c$  (inside network edges) and  $\sigma_{i,j} = 0$  when  $e_{i,j} \notin G_c$  (outside network edges). We simulate 100 data sets at three different settings with different levels of signal to noise ratio (SNR) by using various sample sizes  $n$  and values of  $\rho$ . A larger sample size reduces the asymptotic variance of  $\hat{\sigma}_{i,j}$  and thus the noise level is lower; and a higher absolute value of  $\rho$  represents higher signal level. A higher SNR leads to more distinct empirical distributions of  $\hat{\sigma}_{i,j}$  between inside network edges  $e_{i,j} \in G_c$  and outside network edges  $e_{i,j} \notin G_c$ . Figure 1c demonstrates a calculated correlation matrix based on a simulated data set.

In our simulated data sets, 150 edges are connected and 4800 edges are unconnected, which together represent the graph edge skeleton  $E$ . For both precision matrix shrinkage and covariance matrix thresholding methods we treat a non-zero entry  $\hat{\delta}_{i,j} = 1$  (Mazumder and Hastie, 2012) as a connected edge. We summarize the false positive (FP) edges  $\hat{\delta}_{i,j} = 1$  when the edge is not connected and  $e_{i,j} \notin G_c$  and false negative (FN) edges  $\hat{\delta}_{i,j} = 0$  when the edge is connected and  $e_{i,j} \in G_c$ . We compare FN and FP counts of each method by contrasting the estimated  $\hat{E}$  with the truth  $E$ . We compare our method with *glasso*, CLIME, universal thresholding (Thresh), and adaptive thresholding (AThres) by comparing the FP and FN rates of estimating the graph edge skeleton  $E$ .

## 4.2 Numerical Results

The simulation results are summarized in Table 1. Rather than selecting a single tuning parameter  $\lambda$  for *glasso* and other methods by cross-validation, we explore all possible choices within the reasonable range. Cross the 100 simulation data sets, we summarize the 25%, 50%, and 75% quantiles of the number of FP and FN edges to assess the performance of each method. The results show that the NICE algorithm outperforms the competing methods even when optimal tuning parameters are used (after comparing with the truth) for these methods. One possible reason could be the NICE algorithm thresholds the covariance matrix based on the topological structure rather than

Table 1: Median along with 25% and 75% quantiles of FP and FN

Method	Tuning Par.	$\sigma = 0.5, n = 25$				$\sigma = 0.5, n = 50$				$\sigma = 0.7, n = 25$			
		FP Quantiles		Med.	FN Quantiles	Med.	FP Quantiles		Med.	FN Quantiles	Med.	FP Quantiles	
glasso	0.1	1673	(1648, 1702)	59	(55, 64)	1621	(1591.5, 1640)	44	(40, 46)	1581.5	(1557, 1606)	45.5	(42, 48)
	0.2	1008.5	(989, 1025)	59	(53.5, 64.5)	630	(610, 644)	38	(33.5, 43)	932.5	(920, 955.5)	36	(32, 40)
	0.3	546	(529.5, 560)	56	(48, 63.5)	151	(141, 162.5)	38	(30.5, 43)	500.5	(490, 516)	28	(23.5, 33)
	0.4	211.5	(200.5, 222.5)	60	(50.5, 72)	19	(16, 21)	48.5	(38, 58)	194	(186, 204.5)	24.5	(20, 29)
	0.5	51	(46, 59)	80.5	(66, 96)	1	(0, 2)	82.5	(67, 96.5)	47	(41.5, 54)	28	(22.5, 35)
	0.6	7	(5, 10)	112.5	(97, 125.5)	0	(0, 0)	130	(118.5, 137)	6	(5, 8.5)	41	(31, 51)
	0.7	0	(0, 1)	140	(131.5, 146)	0	(0, 0)	149	(147, 150)	0	(0, 1)	75	(61.5, 89)
	0.8	0	(0, 0)	149	(148, 150)	0	(0, 0)	150	(150, 150)	0	(0, 0)	127	(119.5, 135)
	0.9	0	(0, 0)	150	(150, 150)	0	(0, 0)	150	(150, 150)	0	(0, 0)	149	(149, 150)
	1.0	0	(0, 0)	150	(150, 150)	0	(0, 0)	150	(150, 150)	0	(0, 0)	150	(150, 150)
CLIME	0.1	1082.5	(1047.5, 1108)	56	(48, 64.5)	993.5	(981, 1024)	39	(32, 45.5)	1054	(1021, 1079)	48.5	(40, 56)
	0.2	353	(339.5, 367.5)	79.5	(69, 87.5)	241.5	(231.5, 251.5)	61	(54, 67.5)	345	(328, 359)	70	(59, 78)
	0.3	63	(57, 69)	110	(98.5, 115)	25	(22, 29)	92	(84.5, 100)	64	(59, 68)	98	(87, 103)
	0.4	0	(0, 1)	140	(135, 144)	0	(0, 0)	130	(124, 135)	0	(0, 1)	134	(129, 139)
	0.5	0	(0, 0)	150	(150, 150)	0	(0, 0)	150	(150, 150)	0	(0, 0)	150	(150, 150)
Thres	0.1	2017.5	(1963.5, 2067.5)	0	(0, 2)	1978.5	(1944.5, 2021.5)	0	(0, 0)	2021.5	(1968.5, 2061)	0	(0, 1)
	0.3	1292.50	(1252, 1331)	2	(0, 5)	1249.5	(1220.5, 1288.5)	0	(0, 0)	1293.5	(1251, 1341.5)	1	(0, 3)
	0.5	721.5	(699, 752)	5	(1, 12)	689	(673.5, 721)	0	(0, 1)	722	(693, 756)	3	(1, 10.5)
	0.7	344.5	(325, 360)	14	(7, 26.5)	328.5	(311.5, 349.5)	1	(0, 2)	342.5	(324, 363)	10	(3, 21.5)
	0.9	132	(121, 143.5)	30	(18, 45)	129.5	(121, 142)	3	(1, 7)	133	(123.5, 146)	24	(12, 39.5)
	1.1	41.5	(35, 46)	55.5	(40, 78.5)	40.5	(36.5, 47.5)	10	(4.5, 17)	40	(35.5, 46.5)	49.5	(28, 63)
	1.3	9	(6, 10)	92	(74, 112)	10	(8, 12)	25	(13, 37)	9	(6, 11)	78	(54.5, 89)
	1.5	1	(0, 2)	126	(112.5, 137)	2	(1, 3)	50.5	(32.5, 68)	1	(0, 2)	106	(92.5, 114)
	1.7	0	(0, 0)	145	(138.5, 148)	0	(0, 0)	85.5	(67, 102.5)	0	(0, 0)	132.5	(120.5, 138.5)
	1.9	0	(0, 0)	150	(149, 150)	0	(0, 0)	120.5	(105, 130)	0	(0, 0)	147	(144, 149)
AThres	0.3	2593	(2566.5, 2627.5)	2	(0, 5)	2538.5	(2509.5, 2571)	0	(0, 0)	2594	(2563, 2619)	1	(0, 3)
	0.5	1460	(1421.5, 1486)	5	(1, 12)	1412.5	(1379.5, 1440)	0	(0, 1)	1453	(1419.5, 1491)	3	(1, 10.5)
	0.7	691.5	(667, 717)	14	(7, 26.5)	668.5	(646, 697)	1	(0, 2)	695.5	(665.5, 720)	10	(3, 21.5)
	0.9	271.5	(258, 291.5)	30	(18, 45)	265	(252, 283.5)	3	(1, 7)	270.5	(255.5, 288)	24	(12, 39.5)
	1.1	83	(75, 95)	55.5	(40, 78.5)	85	(75.5, 95.5)	10	(4.5, 17)	82	(74, 89.5)	49.5	(28, 63)
	1.3	18	(15, 21)	92	(74, 112)	22	(18.5, 25.5)	25	(13, 37)	18	(14.5, 22)	78	(54.5, 89)
	1.5	2	(1, 4)	126	(112.5, 137)	4	(3, 6)	50.5	(32.5, 68)	3	(1, 3)	106	(92.5, 114)
	1.7	0	(0, 0)	145	(138.5, 148)	0	(0, 1)	85.5	(67, 102.5)	0	(0, 0)	132.5	(120.5, 138.5)
	1.9	0	(0, 1)	150	(149, 150)	0	(0, 0)	120.5	(105, 130)	0	(0, 0)	147	(144, 149)
	NICE	None	44	(15, 98)	3	(0, 27)	11	(1, 30)	0	(0, 4)	32.5	(13.5, 71)	14

the a universal shrinkage or thresholding strategy. More importantly, our approach is the only method can automatically detect the underlying SBM-RG topological structures. When the graph topological structure does not, the performance of all methods are similar across all settings. The matrix norm loss is not compared, because the community networks are small in size and norm comparison are likely determined by the false positive edges outside network communities. Thus, the numerical results demonstrate that our new method not only provides more accurate estimation of the covariance matrix and the edge set  $E$  than the competing method, but also automatically detects the community networks where highly correlated edges distribute in an organized fashion.

## 5 Data example

We further apply our method to a publicly available mass spectrometry proteomics data set (Yildiz *et al*, 2007). The study collected matrix-assisted laser desorption ionization mass spectrometry (MALDI MS) data sets to obtain the most abundant peptides/proteins in the serum that may distinguish lung cancer cases from matched controls. The study included 182 subjects in the training data set and 106 in the testing data set. The raw data were 288 mass spectra for all subjects, and each raw spectrum consists roughly 70,000 data points. After preprocessing steps including MS registration, wavelets denoising, alignment, peak detection, quantification, and normalization (Chen *et al*, 2009), 184 features are extracted to represent the most abundant protein and peptide features in the serum. Each feature is located at a distinct  $m/z$  value that could be linked to a specific peptide or protein with some ion charges (feature id label). The original paper intended to utilize the proteomics data to enhance disease diagnosis and prediction. In this paper, we estimate the correlation matrix to investigate the relationship between these features. We use the training data set as our input data  $\mathbf{X}_{n \times p}$  and we further estimate the correlation matrix.

We apply our NICE method to estimate the correlation matrix and detect the correlated peptide/protein networks based on the input (Fisher’s Z transformed) sample correlation matrix (2a). First, we calculate the fuzzy logic weight matrix as shown in 2b. The ‘quality and quantity criterion’ is implemented and  $C=39$  is selected, and the procedure is demonstrated in 2c. The network de-

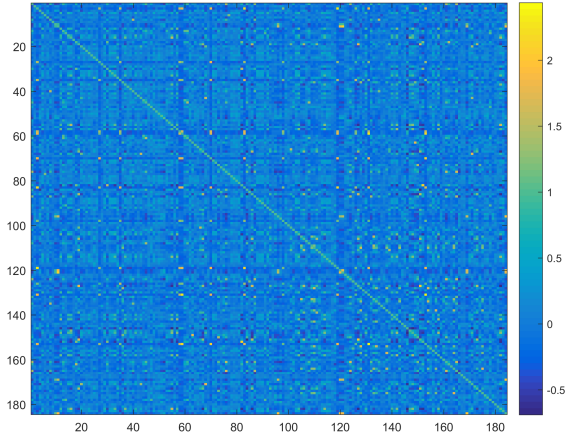


tection is performed to cut edges, allocate correlated features into community networks 2d. Based on the permutation test, six significant networks are detected. Furthermore, inside and outside network edges show distinct distributions of Fisher’s Z transformed correlations 2e. We apply the graph topology oriented adaptive thresholding to estimate  $\hat{E}$  and the correlation matrix 2f. Note that 2e identifies two mixture components: the positively correlated edges and the null, without the negatively correlated edge component. As a result, the negative edges are thresholded. Since the null distribution in 2e seems to be symmetric, based on the Bayes factor decision rule we are confident that edges with relatively high negative correlations are false positive noises. The network detection results provide informative inferences of the interactive relationship between these proteomics features. In this data example, each network represents a group of related protein and peptides that could be confirmed by proteomics mass spectrometry literature. For example, the most correlated network four consists a list of proteins of normal and variant hemoglobins with one and two charges (Lee *et al*, 2011) including normal hemoglobins  $\alpha$  and  $\beta$  with one charge and two charges (at m/z 15127, 15868, 7564, and 7934). The highly correlated networks of biomedical features may potentially provide guidance to detect a set of biomarkers for future research that allow to borrow power between each other.

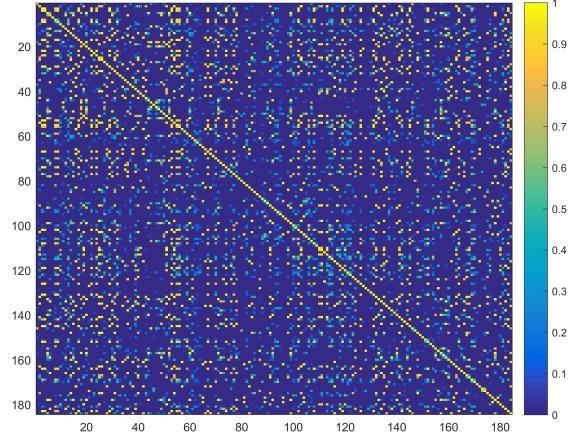
## 6 Discussion and Conclusion

The large covariance/correlation matrices of high-throughput biomedical data sets often exhibit a complex, yet highly organized graph topology reflecting the underlying physiological and biological machinery. However, current regularization methods including shrinkage and thresholding are exploited to estimate the covariance and precision matrix without explicitly utilizing the information from the graph topology. There have been unmet needs of statistical methodologies to uncover the latent topological structure and estimate the correlation matrix with guidance of the topological information. We develop the NICE algorithm to bridge the correlation matrix estimation by incorporating the detected graph topological structure via a flexible empirical Bayesian framework.

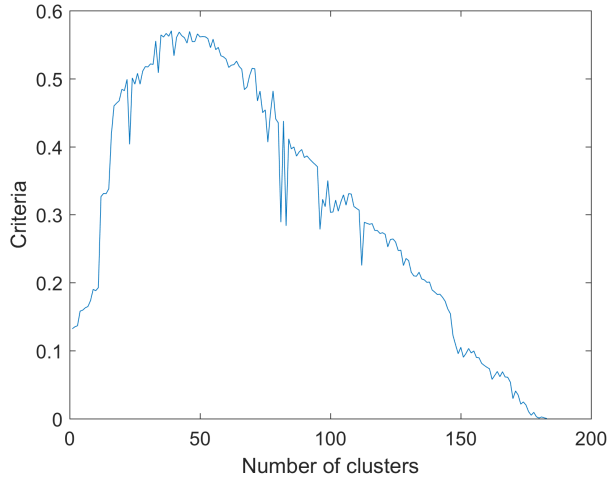
The NICE method makes several contributions. First, We propose a new algorithm to detect



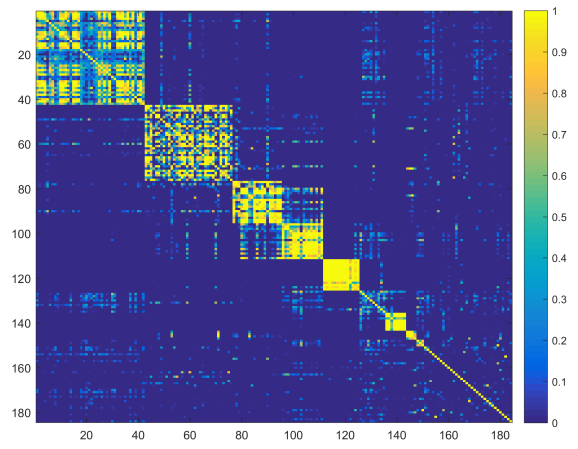
(a) Sample correlation



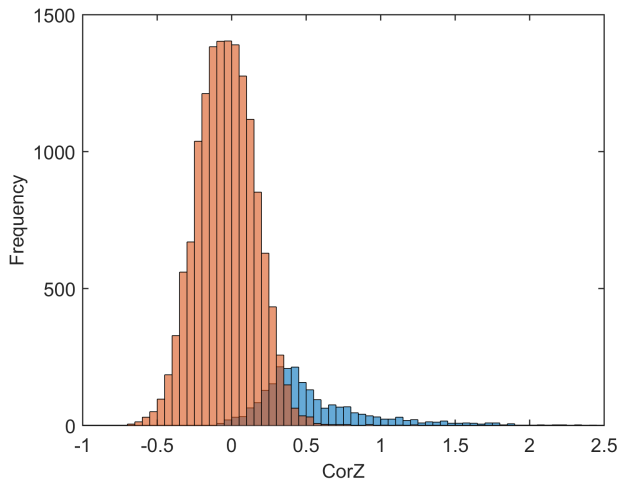
(b) Fuzzy logic weight matrix



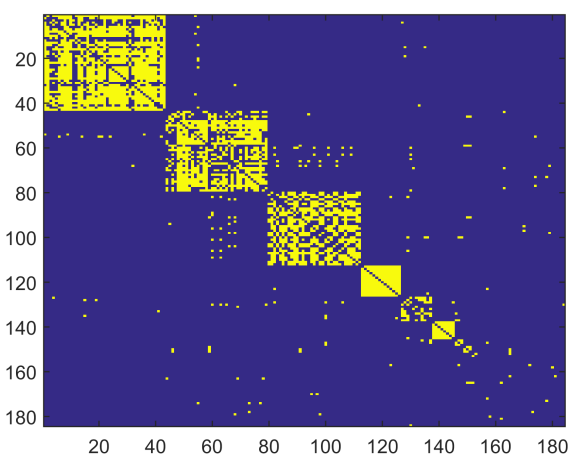
(c) K selection



(d) Network detection: reordered  $W$ .



(e) Edges inside and outside networks



(f) Estimated edge set  $\hat{E}$

Figure 2: Application of the NICE to the example data set.

SBM-RG mixture topological structure. The SBM-RG mixture topological structure is more often observed than the classical SBM in massive data sets from biomedical research. The community detection algorithms (e.g. profile likelihood and modularity maximization for SBM) are often employed to explore the graph topological structures. The results are heavily influenced by two factors: the similarity metrics of the input adjacency matrix and the number of clusters. We develop tailored statistical techniques to yield sensitive and robust similarity matrix and the objective selection of number of clusters to optimally SBM-RG topological structure. Our new fuzzy logic metric provides a sensitive and robust weighted adjacency matrix to better detect the underlying topological structure, which is applicable to general community detection algorithms. Moreover, the ‘quality and quantity’ criterion not only objectively selects the optimal tuning parameter of  $C$ , but also reflects the rule of parsimony because it yields to a few number of significant clusters to contain most informative edges. Note that different from community detection algorithms, our selected tuning parameter  $C$  (by the ‘quantity and quality’ criterion) does not determine the final number of detected networks and a network must pass the permutation test by using the pre-specified statistical significance level. For example, our example data set has  $C=39$  but only six significant networks are detected.

Second, we develop a new Bayes factor based adaptive thresholding technique to naturally incorporate graph topology as prior knowledge. The updated thresholding values are determined by each edge’s ‘location’ on the detected graph topological ‘map’. Therefore, edges borrow strength with each other with higher precision based on detected topological structure, which also provides a flexible pathway to account for the dependency between edges. With additional information from the detected topological structure and appropriate modeling strategy, our new adaptive thresholding method reduces false positive and false negative rates simultaneously when topological structures exist. Clearly, the performance of graph topological structure detection influences the accuracy of correlation matrix thresholding because it determines the empirical distributions of  $z_{i,j}^{in}$  and  $z_{i,j}^{out}$  and thus  $\hat{\theta}_{in}$  and  $\hat{\theta}_{out}$ . Using our ‘quality and quantity’ criterion to select  $C$  maximizes the difference between distributions of edges inside and outside networks, and then the performance of our correlation thresholding is optimal per theory three. Therefore, the parsimonious property of

the ‘quality and quantity’ criterion ensures the parsimony of our following regularization because most edges are outside networks and thus subject to more stringent thresholds. In contrast to the existing  $\ell_1$  shrinkage (e.g. glasso) and thresholding algorithms our NICE algorithm is free of tuning parameter if we adopt the suggested  $T = 4$ . Last but not least, we develop theoretical results to prove the consistency of edge selection and estimation.

In our applications, only positive (correlation) edges are organized in graph topology and the negative (correlation) edges are randomly distributed. Based on the Bayes factor decision rule, none of negative (correlation) edges are suprathrhold. Our methods are also applicable for negatively correlated structure by using absolute values. The numerical studies and example data set application have demonstrated excellent performance of the NICE algorithm. The computational cost of NICE algorithm is low (for our simulation example the algorithm only takes 40 seconds using i7 CPU and 24G memory), and thus it is ready to scale up for larger data sets. In addition, the NICE algorithm is not restricted for multivariate Gaussian distributed data and it is straightforward to extend the sample correlation matrix to other sample metrics, for example maximal information coefficients (Kinney and Atwal, 2014) for continuous data and polychoric correlation coefficient for categorical data (Bonett and Price, 2005) because both fuzzy logic metric and graph topology oriented thresholding are based on the empirical distribution of the coefficients (though new theoretical properties need to be developed for these extensions).

## Acknowledgements

The research is based upon work supported by the Office of the Director of National Intelligence (ODNI), Intelligence Advanced Research Projects Activity (IARPA), via DJF-15-1200-K-0001725.

# A Appendix

## A.1 Proof of Lemma 3.2

*Proof.* For any  $i, j$ , let  $Y_k = X_{i,k}X_{j,k}$ . Then  $Y_1, \dots, Y_n$  are independent and identically distributed. By Condition 3.1,  $P[|Y_k| < M^2] = 1$ . Define

$$z_{i,j} = g(Y_1, \dots, Y_l, \dots, Y_n) = \frac{1}{2} \log \left( \frac{1 + \sum_{k \neq l}^n Y_k/n + Y_l/n}{1 - \sum_{k \neq l}^n Y_k/n - Y_l/n} \right).$$

Then for all  $l = 1, \dots, n$ , by Taylor expansion, we have

$$\begin{aligned} & g(Y_1, \dots, Y_l, \dots, Y_n) - g(Y_1, \dots, Y'_l, \dots, Y_n) \\ &= \sum_{k=1}^{\infty} \frac{\partial^k g}{\partial Y_l^k}(Y_1, \dots, Y'_l, \dots, Y_n) \frac{(Y_l - Y'_l)^k}{k!} \end{aligned}$$

where

$$\frac{\partial^k g}{\partial Y_l^k}(Y_1, \dots, Y'_l, \dots, Y_n) = \frac{(k-1)!}{2n^k} \left( \frac{(-1)^{k+1}}{(1 + \widehat{R}_{i,j})^k} + \frac{1}{(1 - \widehat{R}_{i,j})^k} \right),$$

By Condition 3.1,  $|R_{i,j}| < 1$  and strong law of large number,  $\widehat{R}_{i,j} < 1$  with probability one. Thus, there exists  $N > 0$  and  $K_0 > 0$ , for all  $n > N$ , we have

$$\sup_{Y_1, \dots, Y_n, Y'_l} |g(Y_1, \dots, Y_l, \dots, Y_n) - g(Y_1, \dots, Y'_l, \dots, Y_n)| \leq \frac{K_0}{n}$$

By the McDiarmid inequality, for all  $n \geq N$ , we have

$$P[|z_{i,j} - E[z_{i,j}]| > \epsilon] \leq \exp \left( -\frac{2n\epsilon^2}{K_0^2} \right).$$

Thus,

$$P[\sqrt{n}|z_{i,j} - E[z_{i,j}]| > \epsilon] \leq \exp \left( -\frac{2}{K_0^2} \epsilon^2 \right).$$

Taking  $K = 2/K_0^2 > 0$  completes the proof. □

## A.2 Proof of Lemma 3.4

*Proof.* When  $e_{i,j} \in G$  and  $\mu_{i,j} > 0$ , then

$$\begin{aligned}
& \mathbb{P} \left[ \frac{\sum_{i',j'} \delta_{i',j'}^0 \phi\{\sqrt{n}(z_{i,j} - \mu_{i',j'})\}}{\{p_n(p_n - 1)/2 - q_n\} \phi(\sqrt{n}z_{i,j})} \leq T \right] \\
& \leq \mathbb{P} \left[ \frac{\phi\{\sqrt{n}(z_{i,j} - \mu_{i,j})\}}{\{p_n(p_n - 1)/2 - q_n\} \phi(\sqrt{n}z_{i,j})} \leq T \right] \\
& = \mathbb{P} \left[ -(z_{i,j} - \mu_{i,j})^2 + z_{i,j}^{2(n)} \leq \frac{2}{n} [\log(T) + \log\{p_n(p_n - 1)/2 - q_n\}] \right] \\
& = \mathbb{P} \left[ z_{i,j} \leq \frac{1}{2}\mu_{i,j} + \frac{1}{\mu_{i,j}n} [\log(T) + \log\{p_n(p_n - 1)/2 - q_n\}] \right] \\
& = \mathbb{P} \left[ \sqrt{n}(z_{i,j} - \mu_{i,j}) \leq -\sqrt{n}\mu_{i,j}/2 + \frac{1}{\mu_{i,j}\sqrt{n}} \{\log(T) + \log\{p_n(p_n - 1)/2 - q_n\}\} \right] \\
& \leq \mathbb{P} \left[ \sqrt{n}(z_{i,j} - \mu_{i,j}) \leq -\sqrt{n}\mu_{\inf}/2 + \frac{1}{\mu_{\sup}\sqrt{n}} \{\log(T) + \log(\{p_n(p_n - 1)/2 - q_n\})\} \right],
\end{aligned}$$

where  $\mu_{\sup} = \sup_{i,j} \{|\mu_{i,j}| : e_{i,j} \in G\}$  and  $\mu_{\inf}$  is defined in Condition 3.2. Note that  $\mathbb{E}[z_{i,j}] = \mu_{i,j} + o(n^{-1/2})$ . There exists  $N_2$ , for all  $n > N_2$ , such that  $\sqrt{n}(\mu_{i,j} - \mathbb{E}[z_{i,j}]) < 1$ . Then  $-\sqrt{n}\mathbb{E}[z_{i,j}] - 1 < -\sqrt{n}\mu_{i,j}$  and thus,

$$\begin{aligned}
& \mathbb{P} \left[ \sqrt{n}(z_{i,j} - \mu_{i,j}) \leq -\sqrt{n}\mu_{\inf}/2 + \frac{1}{\mu_{\sup}\sqrt{n}} \{\log(T) + \log(p_n(p_n - 1)/2 - q_n)\} \right] \\
& \leq \mathbb{P} \left[ \sqrt{n}(z_{i,j} - \mathbb{E}[z_{i,j}]) \leq -\sqrt{n}\mu_{\inf}/2 + \frac{1}{\mu_{\sup}\sqrt{n}} \{\log(T) + \log(p_n(p_n - 1)/2 - q_n)\} + 1 \right]
\end{aligned}$$

By Condition 3.2, we have  $\mu_{\inf} = c_0 n^{-1/2+\tau}$  with  $\tau > 0$ , then  $\mu_{\sup} > c_0 n^{-1/2+\tau}$ . Also, by Conditions 3.3 and 3.4, we have  $\log\{p_n(p_n - 1)/2 - q_n\} = o(n^{2\tau})$ , then there exists  $N_1$  such that for all  $n > N_1$  we have  $n^{-\tau} \log\{T(p_n(p_n - 1)/2 - q_n)\} < c_0^2 n^\tau / 8$  and  $n^\tau > 8/c_0$ . By Lemma 3.2,

$$\begin{aligned}
& \mathbb{P} \left[ \frac{\sum_{i',j'} \delta_{i',j'}^0 \phi\{\sqrt{n}(z_{i,j} - \mu_{i',j'})\}}{\{p_n(p_n - 1)/2 - q_n\} \phi(\sqrt{n}z_{i,j})} \leq T \right] \\
& \leq \mathbb{P} \left[ \sqrt{n}(z_{i,j} - \mu_{i,j}) \leq -\frac{c_0}{4} n^\tau \right] \leq \exp \left( -\frac{c_0^2 K n^{2\tau}}{16} \right).
\end{aligned}$$

When  $\mu_{i,j} < 0$ , based on similar arguments, we have

$$\begin{aligned} & \mathbb{P} \left[ \frac{\sum_{i',j'} \delta_{i',j'}^0 \phi\{\sqrt{n}(z_{i,j} - \mu_{i',j'})\}}{\{p_n(p_n - 1)/2 - q_n\} \phi(\sqrt{n}z_{i,j})} \leq T \right] \\ & \leq \mathbb{P} \left[ -\sqrt{n}(z_{i,j} - \mu_{i,j}) \leq -\frac{c_0}{4}n^\tau \right] \leq \exp \left( -\frac{c_0^2 K n^{2\tau}}{16} \right). \end{aligned}$$

Taking  $C_1 = c_0^2 K/16$  completes the proof for the case when  $e_{i,j} \in G$ .

When  $e_{i,j} \notin G$ , then

$$\begin{aligned} & \mathbb{P} \left[ \frac{\sum_{i',j'} \delta_{i',j'}^0 \phi\{\sqrt{n}(z_{i,j} - \mu_{i',j'})\}}{(p_n(p_n - 1)/2 - q_n) \phi(\sqrt{n}z_{i,j})} > T \right] \\ & \leq \mathbb{P} \left[ \frac{q_n \phi\{\sqrt{n}(z_{i,j} - \mu_{\inf}/3)\}}{(p_n(p_n - 1)/2 - q_n) \phi(\sqrt{n}z_{i,j})} > T, |z_{i,j}| \leq \mu_{\inf}/3 \right] \\ & \quad + \mathbb{P} \left[ \frac{\sum_{i',j'} \delta_{i',j'}^0 \phi\{\sqrt{n}(z_{i,j} - \mu_{i',j'})\}}{(p_n(p_n - 1)/2 - q_n) \phi(\sqrt{n}z_{i,j})} > T, |z_{i,j}| > \mu_{\inf}/3 \right] \\ & \leq \mathbb{P} \left[ \sqrt{n}z_{i,j} > \sqrt{n}(\mu_{\inf}/6) + \frac{3}{\mu_{\inf}\sqrt{n}} \log \left( T \times \frac{p_n(p_n - 1)/2 - q_n}{q_n} \right) - 1 \right] + \mathbb{P} [|z_{i,j}| > \mu_{\inf}/3]. \end{aligned}$$

By Condition 3.4,  $\lim_{n \rightarrow \infty} \log\{(p_n(p_n - 1)/2 - q_n)/q_n\} = \pi_0/(1 - \pi_0)$ , there exists  $N_0$  such that for all  $n > N_0$ ,  $\log\{T(p_n(p_n - 1)/2 - q_n)/q_n\} > 0$  and  $n^\tau > 12/c_0$ . Thus,

$$\begin{aligned} & \mathbb{P} \left[ \frac{\sum_{i',j'} \delta_{i',j'}^0 \phi\{\sqrt{n}(z_{i,j} - \mu_{i',j'})\}}{(p_n(p_n - 1)/2 - q_n) \phi(\sqrt{n}z_{i,j})} > T \right] \\ & \leq \mathbb{P} [\sqrt{n}z_{i,j} > c_0 n^\tau/12] + \mathbb{P} [\sqrt{n}|z_{i,j}| > c_0 n^\tau/3] \leq 3 \exp \left( -\frac{c_0^2 K}{144} n^{2\tau} \right). \end{aligned}$$

Taking  $C_0 = c_0^2 K/144$ ,  $C_2 = 3$  and  $N_T = \max\{N_0, N_1, N_2\}$  completes the proof for all the cases.  $\square$

### A.3 Proof Lemma 3.5

*Proof.* Since  $T > (1 - \pi_0)/\pi_0$ . Then there exists  $\epsilon > 0$  such that  $T - \epsilon > (1 - \pi_0)/\pi_0$ . By Lemma 3.3 and Condition 3.4, there exists  $N_1 > 0$ , for all  $n > N_1$  such that

$$\frac{\pi_1 f_1(z_{i,j})}{\pi_0 f_0(z_{i,j})} > \frac{\sum_{i',j'} \delta_{i',j'}^0 \phi\{\sqrt{n}(z_{i,j} - \mu_{i',j'})\}}{(p_n(p_n - 1)/2 - q_n) \phi(\sqrt{n}z_{i,j})} - \epsilon,$$

$$\frac{\pi_1 f_1(z_{i,j})}{\pi_0 f_0(z_{i,j})} < \frac{\sum_{i',j'} \delta_{i',j'}^0 \phi\{\sqrt{n}(z_{i,j} - \mu_{i',j'})\}}{(p_n(p_n - 1)/2 - q_n) \phi(\sqrt{n} z_{i,j})} + \epsilon.$$

Then by Lemma 3.4, when  $e_{i,j} \in G$ , then  $\delta_{i,j}^0 = 1$  and

$$\begin{aligned} \mathbb{P}[\widetilde{\delta}_{i,j}(T) = 0] &= \mathbb{P}\left[\frac{\pi_1 f_1(z_{i,j})}{\pi_0 f_0(z_{i,j})} \leq T\right] \\ &\leq \mathbb{P}\left[\frac{\sum_{i',j'} \delta_{i',j'}^0 \phi\{\sqrt{n}(z_{i,j} - \mu_{i',j'})\}}{(p_n(p_n - 1)/2 - q_n) \phi(\sqrt{n} z_{i,j})} \leq T + \epsilon\right] \leq \exp(-C_1 n^{2\tau}). \end{aligned}$$

when  $e_{i,j} \notin G$ , then  $\delta_{i,j}^0 = 0$  and

$$\begin{aligned} \mathbb{P}[\widetilde{\delta}_{i,j}(T) = 1] &= \mathbb{P}\left[\frac{\pi_1 f_1(z_{i,j})}{\pi_0 f_0(z_{i,j})} > T\right] \\ &\leq \mathbb{P}\left[\frac{\sum_{i',j'} \delta_{i',j'}^0 \phi\{\sqrt{n}(z_{i,j} - \mu_{i',j'})\}}{(p_n(p_n - 1)/2 - q_n) \phi(\sqrt{n} z_{i,j})} > T - \epsilon\right] \leq C_2 \exp(-C_0 n^{2\tau}). \end{aligned}$$

Taking  $C_3 = \max\{1, C_2\}$  and  $C_4 = \min\{C_0, C_1\}$ , thus,

$$\Pr[\widetilde{\delta}_{i,j}(T) \neq \delta_{i,j}^0] \leq C_3 \exp(-C_4 n^{2\tau}).$$

□

## Proof of Lemma 3.6

*Proof.* Since  $T > (1 - \pi_0)/\pi_0$ , then there exists  $\epsilon > 0$  such that  $T - \epsilon > (1 - \pi_0)/\pi_0$ . By Condition 3.5, there exists  $N_0 > 0$ , for all  $n > N_0$  and all  $i, j$  such that

$$\frac{\widehat{\pi}_1 \widehat{f}_1(z_{i,j})}{\widehat{\pi}_0 \widehat{f}_0(z_{i,j})} > \frac{\pi_1 f_1(z_{i,j})}{\pi_0 f_0(z_{i,j})} - \epsilon, \quad \text{and} \quad \frac{\widehat{\pi}_1 \widehat{f}_1(z_{i,j})}{\widehat{\pi}_0 \widehat{f}_0(z_{i,j})} < \frac{\pi_1 f_1(z_{i,j})}{\pi_0 f_0(z_{i,j})} + \epsilon.$$

By Lemma 3.6, When  $e_{i,j} \in G$ , then  $\mathbb{P}[\widehat{\delta}_{i,j}(T) = 0] \leq \mathbb{P}[\widetilde{\delta}_{i,j}(T + \epsilon) = 0] \leq C_3 \exp(-C_4 n^{2\tau})$ , and when  $e_{i,j} \notin G$ , then  $\mathbb{P}[\widehat{\delta}_{i,j}(T) = 1] \leq \mathbb{P}[\widetilde{\delta}_{i,j}(T - \epsilon) = 1] \leq C_3 \exp(-C_4 n^{2\tau})$ . □



## A.4 Proof of Theorem 1

*Proof.* By Lemma 3.6 and the Bonferroni inequality,

$$\begin{aligned} \mathbb{P}\{\widehat{\Delta}(T) \neq \Delta_0\} &= \mathbb{P}\left[\bigcup_{i < j} \{\widehat{\delta}_{i,j}(T) \neq \delta_{i,j}^0\}\right] \\ &\leq \sum_{1 \leq i < j \leq p_n} \mathbb{P}\left[\widetilde{\delta}_{i,j}(T) \neq \delta_{i,j}^0\right] \leq \frac{C_3}{2} p_n(p_n - 1) \exp(-C_4 n^{2\tau}). \end{aligned}$$

By Condition 3.3,  $\lim_{n \rightarrow \infty} p_n(p_n - 1) \exp(-C_4 n^{2\tau}) = 0$ . This completes the proof.  $\square$

## A.5 Proof of Theorem 2

*Proof.* Note that

$$\begin{aligned} &\mathbb{P}[\|\text{NICE}(\widehat{\mathbf{R}}; T) - \mathbf{R}\|_\infty > \epsilon] \\ &= \mathbb{P}[\|\text{NICE}(\widehat{\mathbf{R}}; T) - \mathbf{R}\|_\infty > \epsilon; \widehat{\Delta}(T) = \Delta_0] + \mathbb{P}[\|\text{NICE}(\widehat{\mathbf{R}}; T) - \mathbf{R}\|_\infty > \epsilon; \widehat{\Delta}(T) \neq \Delta_0] \\ &\leq \mathbb{P}\left[\max_{i < j, e_{i,j} \in G} |\widehat{R}_{i,j} - R_{i,j}| > \epsilon\right] + \mathbb{P}[\widehat{\Delta}(T) \neq \Delta_0] \end{aligned}$$

By Bonferroni inequality and Hoeffding's inequality, we have

$$\mathbb{P}\left[\max_{i < j: e_{i,j} \in G} |\widehat{R}_{i,j} - R_{i,j}| > \epsilon\right] \leq \sum_{i < j: e_{i,j} \in G} \mathbb{P}[|\widehat{R}_{i,j} - R_{i,j}| > \epsilon] \leq q_n \exp\left(-\frac{n\epsilon^2}{2M^4}\right).$$

By Conditions 3.3 and 3.4,  $q_n = o(n^{2\tau})$ . Since  $0 < \tau < 1/2$ , then  $\lim_{n \rightarrow \infty} q_n \exp(-n\epsilon^2/2M^4) = 0$ .

By Theorem 1, we have  $\lim_{n \rightarrow \infty} \mathbb{P}[\widehat{\Delta}(T) \neq \Delta_0] = 0$ . This completes the proof.  $\square$

## A.6 Proof of Theorem 3

*Proof.* Applying the universal decision rule with  $z_0$  as threshold:

$$E(\#FP) = m \int_{z_0}^{\infty} \frac{f_0(z)}{\pi_0 f(z)} f(z) dz = m \pi_0 F_0(z_0) = m \omega \pi_0^{in} F_0(z_0) + m(1 - \omega) \pi_0^{out} F_0(z_0) \quad (9)$$

where we denote  $\int_{z_0}^{\infty} f = F(z_0)$ .

For edges in communities:

$$E^{in}(\#FP) = \omega m \int_{z_{in}}^{\infty} \frac{\pi_0^{in} f_0^{in}(z)}{f^{in}(z)} f^{in}(z) dz = \omega m \pi_0^{in} F_0^{in}(z_{in}) \quad (10)$$

For edges outside communities:

$$E^{out}(\#FP) = (1 - \omega) m \int_{z_{out}}^{\infty} \frac{\pi_0^{out} f_0^{out}(z)}{f^{out}(z)} f^{out}(z) dz = (1 - \omega) m \pi_0^{out} F_0^{out}(z_{out}) \quad (11)$$

where  $z_{in} < z_0 < z_{out}$ , and  $F_0^{out}(z) = F_0^{in}(z) = F_0(z)$ . There we expect  $E(\#FP)$  (9)  $> E^{in}(\#FP) + E^{out}(\#FP)$  (10 + 11) if

$$\begin{aligned} & -\omega m \pi_0^{in} (F_0(z_{in}) - F_0(z_0)) + (1 - \omega) m \pi_0^{out} (F_0(z_0) - F_0(z_{out})) > 0, \\ \Leftrightarrow & \frac{F_0(z_0) - F_0(z_{out})}{F_0(z_{in}) - F_0(z_0)} > \frac{\omega \pi_0^{in}}{(1 - \omega) \pi_0^{out}} \end{aligned} \quad (12)$$

On the other hand, we further calculate the expected number of true positive (TP) edges using universal threshold and in/out communities to evaluate the power of our graph topology oriented adaptive thresholding.

Applying the universal decision rule with  $z_0$  as threshold:

$$E(\#TP) = m \int_{z_0}^{\infty} \frac{f_1(z)}{\pi_1 f(z)} f(z) dz = m \pi_1 F_0(z_0) = m \omega \pi_1^{in} F_1(z_0) + m(1 - \omega) \pi_1^{out} F_1(z_0) \quad (13)$$

For edges in communities:

$$E^{in}(\# TP) = \omega m \int_{z_{in}}^{\infty} \frac{\pi_1^{in} f_1^{in}(z)}{f^{in}(z)} f^{in}(z) dz = \omega m \pi_1^{in} F_1^{in}(z_{in}) \quad (14)$$

For edges outside communities:

$$E^{out}(\# TP) = (1 - \omega) m \int_{z_{out}}^{\infty} \frac{\pi_1^{out} f_1^{out}(z)}{f^{out}(z)} f^{out}(z) dz = (1 - \omega) m \pi_1^{out} F_1^{out}(z_{out}) \quad (15)$$

where  $z_{in} < z_1 < z_{out}$ , and  $F_1^{out}(z) = F_1^{in}(z) = F_1(z)$ . There we expect  $E(\# TP)$  (13)  $< E^{in}(\# TP) + E^{out}(\# TP)$  (14 + 15) (i.e.  $E(\# FN) > E^{in}(\# FN) + E^{out}(\# FN)$ ) if

$$\begin{aligned} & -\omega m \pi_0^{in} (F_1(z_{in}) - F_1(z_0)) + (1 - \omega) m \pi_1^{out} (F_1(z_0) - F_1(z_{out})) < 0, \\ \Leftrightarrow & \frac{F_1(z_0) - F_1(z_{out})}{F_1(z_{in}) - F_1(z_0)} < \frac{\omega \pi_1^{in}}{(1 - \omega) \pi_1^{out}} \end{aligned} \quad (16)$$

□

Conditions 3.6 and 3.7 are generally true because our SBM-RG detection algorithm (including the ‘quality and quantity criterions’) and permutation test ensure the communities have high proportions of more correlated edges. We have run numerous empirical experiments and the results further verify the statement. Also, when our ‘quality and quantity’ criteria is optimal that all truly connected edges are included in the detected networks and all networks exclusively include truly connected edges, the our adaptive thresholding method ensures perfect detection of truly connected edges with zero false positive discovery. If the assumption of network induced covariance is true, the  $C$  selection procedure chooses the parameter to optimize the ‘quality and quantity’ criteria that allows to reduce false positive findings and improve power simultaneously.

## A.7 Convenient thresholding value calculation

We calculate the thresholding values for edges inside-networks and outside-networks separately, and the cut-off can be linked to the overall local  $fdr$  value. Therefore, the computation is more straightforward by using the following cut-offs.

For edges inside networks we would use your local  $fdr$  cut-off as  $1/(T + 1)$ ,

$$\begin{aligned} \frac{\pi_1^{in} f_1(z)}{\pi_0^{in} f_0(z)} &= (1 - fdr^{in})/fdr^{in} = T \\ \Leftrightarrow \frac{f_1(z)}{f_0(z)} &= T \frac{\pi_0^{in}}{\pi_1^{in}} \end{aligned} \quad (17)$$

and if  $\frac{f_1(z)}{f_0(z)} > T \frac{\pi_0^{in}}{\pi_1^{in}}$  we consider the edge is truly connected.

The above cut-off is equivalent to the cut-off for all edges inside and outside the networks by applying the decision rule of  $\frac{f_1(z)}{f_0(z)} > 4 \frac{\pi_0^{in}}{\pi_1^{in}}$ :

$$\begin{aligned} \frac{\pi_1^{all} f_1(z)}{\pi_0^{all} f_0(z)} &= (1 - fdr^{all})/fdr^{all} \\ \Leftrightarrow \frac{f_1(z)}{f_0(z)} \frac{\pi_1^{all}}{\pi_0^{all}} &= T \frac{\pi_0^{in}}{\pi_1^{in}} \frac{\pi_1^{all}}{\pi_0^{all}} = (1 - fdr^{all})/fdr^{all} \\ \Leftrightarrow fdr^{all}(in) &= \frac{1}{T \frac{\pi_0^{in}}{\pi_1^{in}} \frac{\pi_1^{all}}{\pi_0^{all}} + 1} \end{aligned} \quad (18)$$

For example, if  $\pi_0^{in}/\pi_1^{in} = 10$  and  $\pi_1^{all}/\pi_0^{all} = 10$ , then  $fdr^{all}(in)=0.96$  and most edges are not thresholded as the cut-off is loose.

Similarly, for edges outside networks

$$fdr^{all}(out) = \frac{1}{T \frac{\pi_0^{out}}{\pi_1^{out}} \frac{\pi_1^{all}}{\pi_0^{all}} + 1}$$

if  $T = 4$ ,  $\pi_0^{out}/\pi_1^{out} = 40$  and  $\pi_1^{all}/\pi_0^{all} = 0.1$ , then  $fdr^{all}(out)=0.06$  and most edges outside the network are thresholded by using a more stringent cut-off.

When the data shows no network structure, for instance,  $\pi_0^{in}/\pi_1^{in} = \pi_0^{out}/\pi_1^{out} = 10$  and  $\pi_1^{all}/\pi_0^{all} = 10$ , then  $fdr^{all}(in) = fdr^{all}(out) = 0.2$ . Our adaptive thresholding rule boils down to the universal thresholding rule.

## References

- Banerjee, O., El Ghaoui, L. and d’Aspremont, A. (2008). Model selection through sparse maximum likelihood estimation for multivariate Gaussian or binary data. *The Journal of Machine Learning Research* **9**, 485-516.
- Besag, J., Kooperberg, C. (1995). On conditional and intrinsic autoregressions. *Biometrika*, **82**(4), 733-746.
- Bickel, P.J., Levina, E. (2008). Covariance regularization by thresholding. *Ann. Statist.* **36**, no. 6, 2577–2604.
- Bickel, P. J., Chen, A. (2009). A nonparametric view of network models and NewmanGirvan and other modularities. *Proceedings of the National Academy of Sciences*, **106**(50), 21068-21073.
- Bonett, D. G., Price R. M. (2005). Inferential Methods for the Tetrachoric Correlation Coefficient. *Journal of Educational and Behavioral Statistics*, **30**, 213.
- Cai, T., Liu, W. and Luo, X. (2011). A constrained  $\ell_1$  minimization approach to sparse precision matrix estimation. *Journal of the American Statistical Association*, **106**, 594–607.
- Cai, T., Liu, W. (2011). Adaptive thresholding for sparse covariance matrix estimation. *J. Amer. Statist. Assoc.* **106** (494), 672–684.
- Cai, T. T., Ren, Z., Zhou, H. H. (2014). Estimating structured high-dimensional covariance and precision matrices: Optimal rates and adaptive estimation. *The Annals of Statistics*, **38**, 2118-2144.
- Chen, S., Li, M., Hong, D., Billheimer, D., Li, H., Xu, B. J., Shyr, Y. (2009). A novel comprehensive wave-form MS data processing method. *Bioinformatics*, **25**(6), 808-814.

- Chen, S., Kang, J., Wang, G. (2015). An empirical Bayes normalization method for connectivity metrics in resting state fMRI. *Frontiers in neuroscience*, **9**, 316-323.
- Chen, S., Kang, J., Xing, Y., Wang, G. (2015). A parsimonious statistical method to detect group-wise differentially expressed functional connectivity networks. *Human brain mapping*, **36**(12), 5196-5206.
- Choi, D. S., Wolfe, P. J., Airolidi, E. M. (2012). Stochastic blockmodels with a growing number of classes. *Biometrika*, **99**, 273-284.
- Chung, F. R. (1997). Spectral Graph Theory (CBMS Regional Conference Series in Mathematics, No. 92), American Mathematical Society.
- Cui, Y., Leng, C., Sun, D. (2016). Sparse estimation of high-dimensional correlation matrices. *Computational Statistics & Data Analysis*, **93**, 390-403.
- Donoho, D. L., Johnstone, I. M., Kerkycharian, G. and Picard, D. (1995). Wavelet shrinkage: asymptopia? (with discussion). *Journal of the Royal Statistical Society, Series B* **57**, 301-369.
- Efron, B. (2004). Large-Scale Simultaneous Hypothesis Testing: The Choice of a Null Hypothesis. *Journal of the American Statistical Association*, **99**, 96-104.
- Efron, B. (2007). Size, power and false discovery rates. *The Annals of Statistics*, **35**(4), 1351-1377.
- Efron, B., Turnbull, B., Narasimhan, B. (2008). locfdr: Computes local false discovery rates. *R package*, 195.
- El Karoui, N. (2010). High-dimensionality effects in the markowitz problem and other quadratic programs with linear constraints: risk underestimation. *The Annals of Statistics*, **38**, 3487-3566.
- Fan, J., Liao, Y., Mincheva, M. (2013). Large covariance estimation by thresholding principal orthogonal complements. With 33 discussions by 57 authors and a reply by Fan, Liao and Mincheva. *J. R. Stat. Soc. Ser. B. Stat. Methodol.* **75**, no. 4, 603-680.
- Fan, J., Liao, Y., Liu, H. (2015). Estimating Large Covariance and Precision Matrices. arXiv preprint arXiv:1504.02995.

- Friedman, J., Hastie, T., Tibshirani, R. Sparse inverse covariance estimation with the graphical lasso. (2008). *Biostat.* **9**(3), 432–441.
- Friedman, J., Hastie, T., Tibshirani, R. (2010). Applications of the lasso and grouped lasso to the estimation of sparse graphical models (pp. 1-22). Technical report, Stanford University.
- Lam, C. and Fan, J. (2009). Sparsistency and rates of convergence in large covariance matrix estimation. *Annals of statistics* **37** 42-54.
- Lee, B. S., Jayathilaka, G. L. P., Huang, J. S., Vida, L. N., Honig, G. R., Gupta, S. (2011). Analyses of in vitro nonenzymatic glycation of normal and variant hemoglobins by MALDI-TOF mass spectrometry. *Journal of biomolecular techniques: JBT*, **22**(3), 90.
- Lei, J., Rinaldo, A. (2014). Consistency of spectral clustering in stochastic block models. *The Annals of Statistics*, **43**(1), 215-237.
- Liu, H., Wang, L. and Zhao, T. (2014). Sparse covariance matrix estimation with eigenvalue constraints. *Journal of Computational and Graphical Statistics*, **23**, 439-459.
- Jeffreys, H. (1961). Theory of Probability, 3rd ed. Clarendon Press, Oxford.
- Kass, R. E., Raftery, A. E. (1995). Bayes factors. *Journal of the american statistical association*, **90**(430), 773-795.
- Karrer, B., Newman, M. E. (2011). Stochastic block models and community structure in networks. *Physical Review E*, **83**(1), 016107.
- Kinney, J. B., Atwal, G. S. (2014). Equitability, mutual information, and the maximal information coefficient. *Proceedings of the National Academy of Sciences*, **111**(9), 3354-3359.
- Mazumder, R. and Hastie, T. (2012). Exact covariance thresholding into connected components for large-scale graphical lasso. *The Journal of Machine Learning Research*, **13**(1), 781-794.
- Nadakuditi, R. R., Newman, M. E. (2012). Graph spectra and the detectability of community structure in networks. *Physical review letters*, **108**(18), 188701.

- Rothman, A. J., Levina, E. and Zhu, J. (2009). Generalized thresholding of large covariance matrices. *Journal of the American Statistical Association* **104**, 177-186.
- Qi, H. and Sun, D. (2006). A quadratically convergent newton method for computing the nearest correlation matrix. *SIAM journal on matrix analysis and applications* **28** 360-385.
- Scott, J. G., Berger, J. O. (2006). An exploration of aspects of Bayesian multiple testing. *Journal of Statistical Planning and Inference*, **136**(7), 2144-2162.
- Scott, J. G., Berger, J. O. (2010). Bayes and empirical-Bayes multiplicity adjustment in the variable-selection problem. *The Annals of Statistics*, **38**(5), 2587-2619.
- Schäfer, J., Strimmer, K. (2005). A shrinkage approach to large-scale covariance matrix estimation and implications for functional genomics. *Statistical applications in genetics and molecular biology*, **4**(1).
- Shen, X., Pan, W. and Zhu, Y. (2012). Likelihood-based selection and sharp parameter estimation. *Journal of the American Statistical Association* **107** 223232.
- Shi, J., Malik, J. (2000). Normalized cuts and image segmentation. *Pattern Analysis and Machine Intelligence, IEEE Transactions on*, **22**(8), 888-905.
- von Luxburg, U. A tutorial on spectral clustering. (2007), *Stat. Comput.* **17** (4), 395–416.
- Witten, D. M., Friedman, J. H., Simon, N. (2011). New insights and faster computations for the graphical lasso. *Journal of Computational and Graphical Statistics*, **20**(4), 892-900.
- Wu, B., Guan, Z., Zhao, H. (2006). Parametric and nonparametric FDR estimation revisited. *Biometrics*, **62**(3), 735-744.
- Yildiz, P. B., Shyr, Y., Rahman, J. S., Wardwell, N. R., Zimmerman, L. J., Shakhtour, B., ... Massion, P. P. (2007). Diagnostic accuracy of MALDI mass spectrometric analysis of unfractionated serum in lung cancer. *Journal of thoracic oncology*, **2**(10), 893-915.
- Yuan, M. and Lin, Y. (2007). Model selection and estimation in the gaussian graphical model. *Biometrika*, **94**, 19–35.



- Yuan, M. (2010). High dimensional inverse covariance matrix estimation via linear programming. *Journal of Machine Learning Research*, **11**, 2261-2286.
- Zhang, C.-H. (2010). Nearly unbiased variable selection under minimax concave penalty. *The Annals of Statistics*, 894942.
- Zhao, Y., Levina, E., Zhu, J. (2011). Community extraction for social networks. *Proceedings of the National Academy of Sciences*, **108**(18), 7321-7326.